Recent Advances in Fault Diagnosis Techniques for Photovoltaic Systems: a Critical Review

Bo Yang, Ruyi Zheng, Yiming Han, Jianxiang Huang, Miwei Li, Hongchun Shu, Shi Su, and Zhengxun Guo

***Abstract*—If a failure in the components of a photovoltaic (PV) system, such as PV module, controller, inverter, load, cable, etc. goes undetected and uncorrected, it can seriously affect the efficiency, safety, and reliability of the entire PV power plant. In addition, fires can occur if specific faults, such as arc, ground, and line-to-line faults remain unresolved. Therefore, PV system (PVS) fault diagnoses are crucial for PV power plant reliability, efficiency, and safety. Many fault diagnosis methods and techniques for PVS components have been developed. In addition, with the development of PV devices, more advanced and intelligent diagnostic technologies are continuously being researched and developed. However, a systematic and thorough analysis, summary, and conclusion are still urgently required. Thus, this paper introduces the types, causes, and impacts of PVS faults, and reviews and discusses the methods proposed in the literature for PVS fault diagnosis, and in particular, failures in PV arrays. Special attention is paid to the optimization direction of various fault diagnosis methods under different priorities, and their limitations, feasibility, complexity, and cost-effectiveness. Finally, challenges and suggestions are put forward for future research.**

***Index Terms*—PVS, monitoring system, PV fault types, PV diagnosis, review.**

NOMENCLATURE

Abbreviations

ABC-SS	artificial bee colony and semi-supervised ELM
AF	arc fault
AIT	artificial intelligence technology
ART	adaptive resonance theory
AWPSO	adaptive weighted particle swarm optimization
BAM	bidirectional associative memory
BP	back propagation
CSM	circuit structure method
CTCT	complex-total-cross-tied
ECM	earth capacitance measurement
EMI	electromagnetic induction
EVA	ethylene-vinyl acetate
FCAM	Fuzzy control algorithm method
FCM	fuzzy c-means
FD	fault diagnosis
FM	fuzzy membership
GF	ground faults
GKFCM	Gaussian kernel FCM
HS	hot spot
HSF	HS faults
IIAM	infrared image analysis method
IVCA	I-V characteristic analysis
LID	light-induced degradation
LLF	line-line fault
LSTM	long short-term memory
MMM	mathematical model method
MOSFET	metal-oxide-semiconductor field-effect transistor
NNM	neural network methods
PID	potential induced degradation
PN	pseudo-noise
PNN	probabilistic neural network
PSO	particle swarm optimization
PV	photovoltaic
PVA	PV array
PVS	PV system
RBF	radial basis function
SOA	seagull optimization algorithm
SP	series-parallel
SRF	stacking random forest
SSPA	statistical and signal processing approaches
SSTDR	spread-spectrum time domain reflection
SVM	support vector machine
TDR	time domain reflectometry

Received: August 19, 2023
Accepted: December 23, 2023
Published Online: May 1, 2024

Yiming Han (corresponding author) is with the School of Faculty of Electric Power Engineering, Kunming University of Science and Technology, Kunming 650500, China (e-mail: kmhym1993@sina.com).

DOI: 10.23919/PCMP.2023.000583

I. INTRODUCTION

In the modern era, the continued consumption of global fossil resources [1], [2] and the environmental threats posed by their usage [3], [4] have become sig-

nificant challenges to human survival. Consequently, renewable energy [5], [6] has emerged as promising for managing the energy crisis [7], [8]. Among the types of renewables, one of the most crucial new energy sources is photovoltaic (PV) power generation. China's total grid-connected PV capacity is expected to reach 392 GW by 2022, comprising 234.4 GW of centralized PV power stations and 157.6 GW of distributed PV power stations. Figure 1 displays the latest global annual PV installed capacity from 2016–2022. Renewable energy resources such as solar energy are relatively inexpensive and non-depletable, so the real challenge lies in overcoming the technology obstacles and the cost associated with developing and utilizing these resources [9]. To enhance the efficiency and economy of PV power generation, researchers have developed various approaches, including optimizing the composition materials of PV modules to improve their conversion rate. From the first generation of silicon-based PV modules to the second generation of multi-component film modules and to the third generation of new material PV modules [10], research has made significant progress in improving their efficieny. Also, by promptly identifying the faults of PVS and performing fault diagnosis and remediation, energy and economic losses can be minimized.

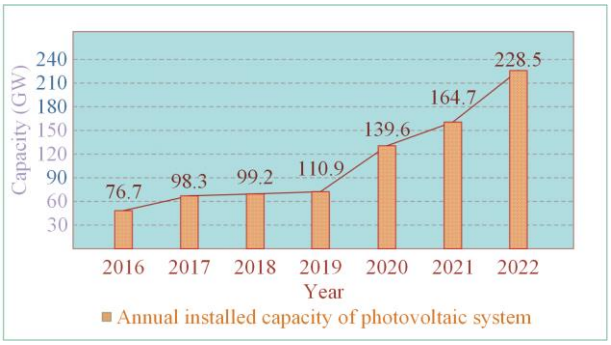

Fig. 1. Global new PV installed capacity from 2016 to 2022.

While several different types of faults can occur in PV arrays (PVA), such as line-line fault (LLF), ground fault (GF), and arc faults (AF) [11], hot spot faults (HSF) are also of significant concern. If not detected in time, an HSF can permanently damage PV cells [12]. In addition, if other faults, such as LLF, AF, HSF, and GF, are not discovered quickly, they can result in hazardous fires. Work has been done to address this hazard [13], and fire prevention measures have been developed [14]. For instance, one study has used an end cloud architecture and imaging to create an early fire warning system for PV power stations

It is important to differentiate between PV fault diagnosis and PV fault detection. The former involves determining the type and location of the fault, while the latter verifies the fault's occurrence based on the difference between measured and calculated data [15]. The study in [16] analyzes the mechanism and fault characteristics of DC fault arcs, and summarizes the detection and location methods of DC fault arcs in PV power generation systems. Reference [12] provides more comprehensive analysis and outlines the causes and effects of the four main faults (LLF, GF, AF, HSF) and their corresponding traditional and advanced fault diagnosis technologies. PVA fault diagnosis is described from the two aspects of a conventional diagnosis method and intelligent algorithm. The latter is clarified not in accordance to the fault type but rather based on the fault diagnosis method [17].

This paper provides an overview of the various electrical methods for diagnosing faults in PVS and briefly introduces non-electrical diagnostic methods. Eight fault diagnosis methods are categorized into four groups, and the practical applications, diagnosis accuracy, diagnostic diversity, complexity, advantages, and disadvantages of all methods are thoroughly compared and evaluated. The paper primarily focuses on the composition of PVS and the causes and effects of the seven significant faults, i.e., PV module, inverter, junction box, and by-pass diode faults, GF, LLF, and AF. It also provides suggestions for the future development of PV fault diagnosis technology.

The paper is structured as follows. Section II provides a comprehensive overview of PVS fault diagnosis methods, and Section III discusses the possible types of faults that may occur on the DC and AC sides of PVS. In Section IV, the FD method proposed for PVS is reviewed and discussed. Section V summarizes and discusses various PV fault diagnosis technologies. Finally, Section VI outlines the challenges, recommendations, and future trends of PV fault diagnosis technology.

II. Review Screening Methods

This paper embarks on a rigorous research approach to present a comprehensive overview of PVS fault diagnosis methods, including their diagnostic technology, performance advantages, and diagnosis direction. Four keywords (PVS, monitoring system, PV fault types, PV diagnosis) were chosen as the basis for conducting an exhaustive literature review using three representative search engines. The title, summary, and keywords were reviewed to curate the most pertinent references, resulting junction box, and by-pass diode faults, GF, LLF, and AF. It also provides suggestions for the future development of PV fault diagnosis technology. And 103 pieces of literature were selected based on citations and journal impact factors.

To better understand the implementation process of the reference review and selection method, a detailed diagram is given in Fig. 2(a) to provide a comprehensive view of the review process. Additionally, statistical data on research in this field over the past seven years (2016–February 2023) were collected from platforms such as Science Direct, Web of Science, and Google

scholar, and are presented in Fig. 2(b), which offers insights into the latest developments in the field.

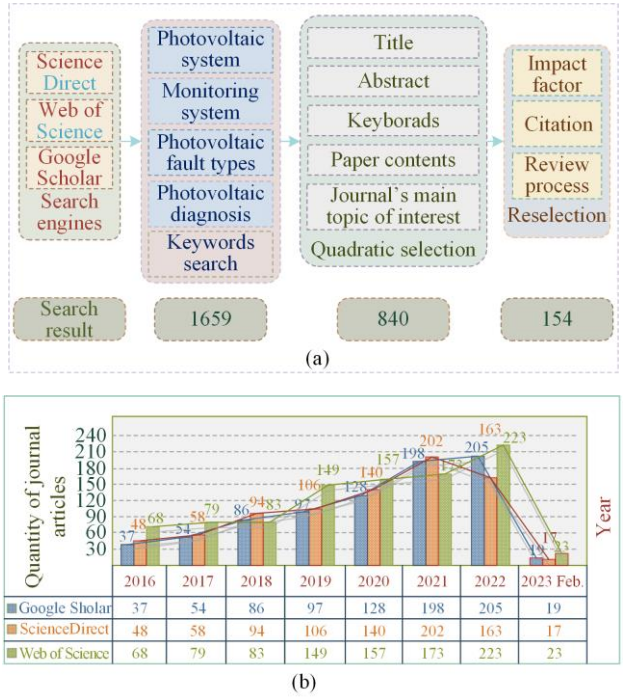

Fig. 2. Review screening methods of related references. (a) Execution procedure. (b) Research statistics.

III. Type of Faults

PVS can be configured in three types: independent, grid-connected, and distributed PV power generation systems. They are comprised of a variety of components, including PV modules, controllers, inverters, loads, and cables. The PV modules generate electricity, which is then sent to the controller to be distributed to the load or battery, depending on the system configuration. The transmission process is varied, e.g., DC is directly sent to DC load, while DC is converted into AC through the inverter to supply to AC load. If the local demand is low, some power can be stored in a battery, serving as back-up energy when the PV power generation is low. The structure diagram of this process is shown in Fig. 3.

PVS is prone to failure, and this can significantly impact the power generation efficiency and power quality, and even lead to fires. Two types of faults can happen in the PV module: permanent and temporary faults. Permanent faults include ethylene-vinyl acetate (EVA) discoloration, layering, hot spots, potential-induced degradation (PID), light-induced degradation (LID), etc. On the other hand, temporary faults usually only require the removal of obstacles, such as shading and soiling [18]. In addition, the faults of PVS are diverse and can be intricated to diagnose. Table I provides an overview of the primary faults of PVS. The failure pictures of PVS are shown in Fig. 4.

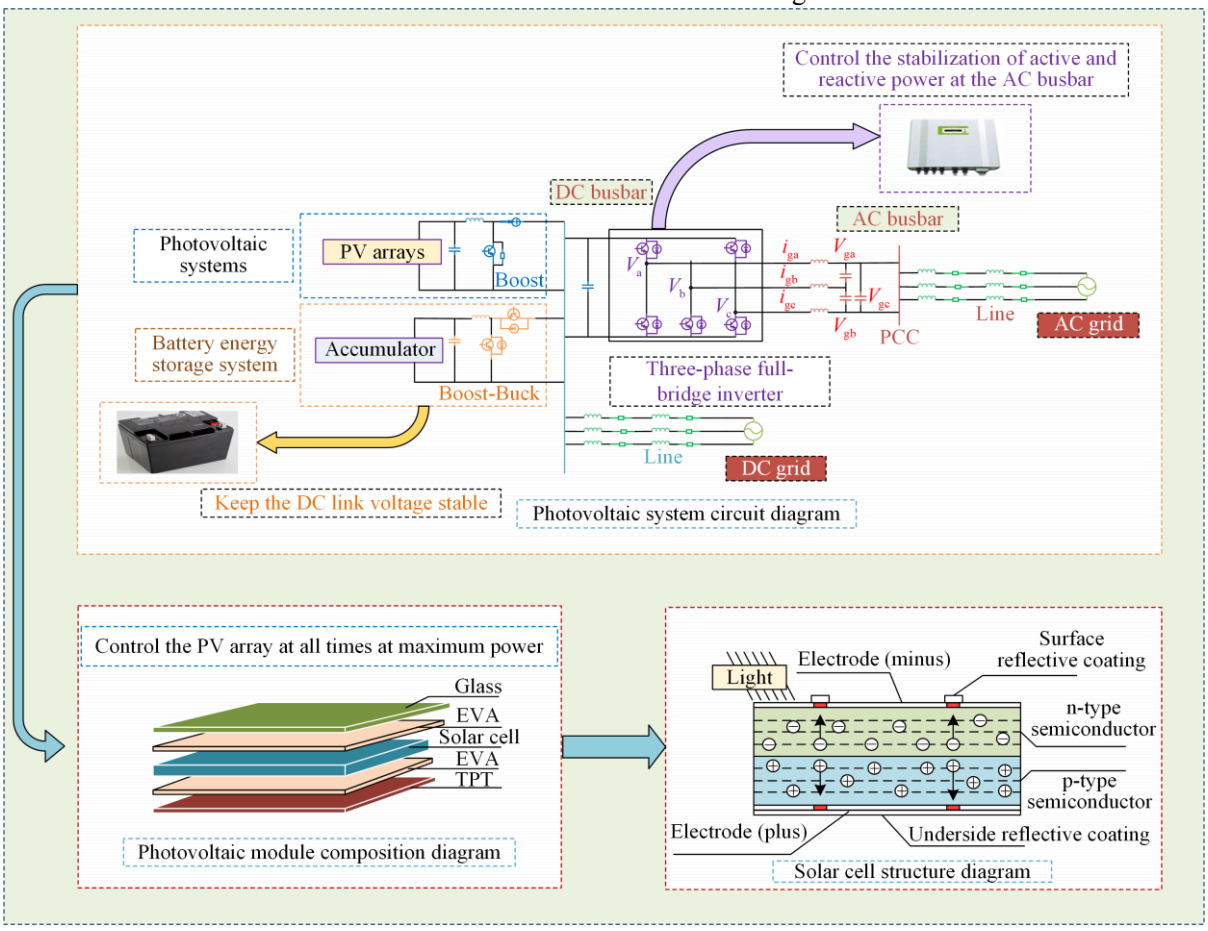

Fig. 3. PVS composition diagram.

TABLE I
SUMMARY OF DIFFERENT TYPES OF FAULTS WITH RELATED INFORMATION

Type of faults		Causes	Effects	Recoverability	Severity
PV module failures modes	EVA discoloration	● High temperature and high humidity environment. ● The additive formula is unstable.	● Shorten the life of PV modules. ● Reduce the efficiency of PV modules. ● Leads to stratification. ● Accelerate the attenuation of PV modules.	Damage caused by discoloration is irreversible.	***
	Delamination	● Foreign objects are on the surface of raw materials, such as EVA, glass, and backplanes. ● The flux is too small, and the main gate line delamination occurs when it encounters high temperatures outside for a long time. ● The variable composition of EVA raw materials (ethylene, vinyl acetate, etc.) leads to insolubilty at room temperature, resulting in delamination. ● The degree of cross-linking is unqualified (such as the low temperature of the film applicator, short film application time, etc.).	● The small layered area affects the battery module's high-power failures. ● When the layered area is large, it will cause the battery module to fail and it then needs to be scrapped.	Permanent losses and irreversible.	***
	HS	● Mixing of individual bad batteries. ● Electrode solder lug virtual welding. ● The storm evolves from cracks to breaks. ● Individual battery. Characteristics deteriorate. ● Shadows partially obscure the battery.	● Reduce the output power. ● Shorten the life of PV modules. ● Burn the components. ● Cause fire.	Many occlusions cause hot spots to be reversible.	****
	PID	● Humid environment. ● The component's surface is contaminated with conductive, acidic, alkaline, and ionic objects. ● The attenuation phenomenon occurs, resulting in the generation of leakage current.	● Attenuate the power of PV modules. ● Shorten the life of PV modules.	It can be repaired in parallel with the inverter DC input by adding a PID repair device.	**
	LID	● Impurities and defects in the battery. ● High temperature. Environment.	● Attenuate the power of PV modules. ● Shorten the life of PV modules.	Can be repaired within a certain period.	**
	Shading and soiling	● Such as gas, dust, and another occlusion.	● Affect the efficiency of PV modules. ● It may cause hot spots.	As long as the obstruction is removed, the fault can be eliminated.	**
Inverter failure modes		● Over-voltage, over-current, over-temperature. ● Over-voltage, harmonic current, high temperature, rapid charge, and discharge. ● The fan's power supply is damaged, or foreign objects enter the fan.	● Cause significant energy loss in PVS.	Depending on where the failure occurred, it is divided into recoverable failures and non-recoverable failures.	***
Bypass diode failures		● The reverse voltage is too large, resulting in an electrical breakdown. ● Exceeding the junction temperature range.	● Cause abnormal appearances such as peeling of packaging materials and melting of backplanes. ● The junction box is deformed or even melted by heat. Cause fire.	No current passage can be recovered in the thermal breakdown, and electrical breakdown is irreversible.	****
Junction box failures		● Component welding process quality problems. ● Component sealing process quality problems. ● Shadow occlusion, cracks, and other issues. ● Lightning strike.	● Reduce the efficiency and reliability of PVS. ● Cause damage and fire.	It needs to be disassembled and repaired.	****
Ground faults		● Cable insulation damage caused by aging, corrosion, or animal bites. ● Ground fault inside the PV module. ● Unexpected short circuit between the conductor and the earth.	● DC power supply short circuit. ● The switch burns out. ● Inverter failure. ● Causes fire.	Divided into recoverable and non-recoverable faults; recoverable faults are automatically eliminated.	**** *
Line-line faults		● Cable insulation damage caused by aging, corrosion, or animal bites.	● Reduce the efficiency and reliability of PVS. ● Cause damage and fire.	It takes a certain amount of time to recover.	****
Arc faults		● Loose terminal block. ● Aging, line insulation skin rupture.	● Causes fire.	It takes a certain amount of time to recover.	****

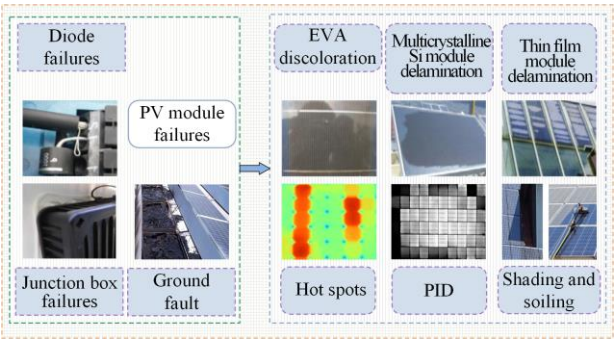

Fig. 4. PVS fault type diagram.

A. PV Module Failures Modes

PV modules (or solar panels) are the core and most pivotal components of PV power generation systems. The quality of PV modules determines the quality of PV power stations, and is the determining factor in the effective and stable operation of the power stations for their lifetime of 25 years.

1) EVA Discoloration

Polymer encapsulants manufactured from EVA copolymers are extensively used in crystalline silicon (c-Si) PV modules for component packaging [19]. Chemically, EVA discoloration is affected by multiple factors, among which formulation additives and curing conditions have significant impact, as they create synergistic chromophores from additives and curing products that lead to increased discoloration rates [20]. Antioxidants, on the other hand, play a vital role in suppressing chromophore production [21]. EVA discoloration is a severe and permanent fault of PVS, resulting in a significant decrease in module power output [22].

2) Delamination

Delamination can significantly affect the performance and reliability of PV modules [23]. When the layered area is small, it will affect the high-power failure of the battery module, and when the layered area is large, it will directly lead to the failure and scrapping of the battery module. Step-heated active infrared thermography can detect and characterize defects in PV modules [24]. Delamination is a permanent failure and cannot be recovered from. So once it occurs, the PV module needs to be replaced.

3) Shading and Soiling

In the field of PV technology, shadows can be caused by pollution, manifesting as either soft shadows, such as those caused by air pollution like smog, or hard shadows, resulting from accumulated dust or solid objects like buildings obstructing the passage of sunlight. Both types can significantly impact the performance and reliability of PV modules [25]. Soft shadows, for example, may affect the current supplied by the module while the voltage remains stable. Conversely, hard shadows may not affect the current but can cause a significant reduction in voltage. It is worth noting that both soft and hard shadows can lead to reduced performance of the PV module. Therefore, it is necessary to develop effective strategies to mitigate the effects of shadowing on performance.

4) Hot Spots

The distribution of cell surface temperatures in solar cells operating in reverse bias mode is not uniform. This can lead to the emergence of local hot spots [26], posing significant reliability issues in PV panels, particularly when cells with different characteristics are joined together. This leads to mismatches that cause the cells to overheat and consequently reduces overall panel performance. High temperatures induced by hot spots can cause permanent damage to PV panels, and this can induce harm to cell encapsulants or even result in secondary breakdown [27].

While bypass diodes are used for protection and can mitigate hot spots, they do not entirely prevent them nor the damage caused [28]. Thus, the presence of hot spots puts PV module lifetime and operational efficiency at risk. When evaluating whether a module is defective, two factors are considered: the temperature difference between the hot spot and the surrounding area and the voltage difference between the affected and unaffected PV modules. Both criteria are crucial for determining the extent of the defect and whether the module needs to be replaced [29].

5) Potential Induced Degradation

Generally, leakage current flows from the module frame to the solar cell because of the potential difference, resulting in PID [30]. PID has become one of the most crucial aspects impacting PV modules and system overall performance and efficacy in recent years. In practice, PID can significantly impact solar power plants, leading to a minimum of 50% reduction in power generation. Bound to occur in the boundary cells of PV modules, PID is heavily influenced by factors such as voltage, temperature, humidity, and grounding mode. These are significant drivers of this phenomenon [31], [32]. Therefore, experts have advocated for various preventative measures, including optimizing the production process, carefully selecting the appropriate materials, and implementing specialized systems for PV modules [33].

However, in addition to preventative measures, appropriate PID recovery measures can be taken, often through standard methods such as negative electrode grounding for the centralized inverter, single point grounding for parallel connection of series inverters, and PID night compensation methods. With such measures in place, it is possible to prevent PID and recover from its harmful effects [32].

6) Light-induced Degradation

LID is a natural phenomenon resulting from the physical reactions of the p-n junction of PV cells [34]. LID causes reduction in the short circuit current and

open circuit voltage of solar cells. The existing recognition of LID effects is mainly divided into two phenomena: Bo-LID and Cu-LID. These two phenomena differ in their distinct characteristics and the defects they form. Bo-LID, for instance, presents itself with a rapid decay initially, followed by a slower decay rate. Bo-LID is entirely reversible if the solar cell is heated to 200 °C. Bo-LID and Cu-LID, as mentioned earlier, involve distinct degradation reactions that produce separate recombinant activity defects [35].

B. Inverter Failure Modes

The PV inverter is a device that converts the variable DC generated by PV panels to AC that can be fed back to a utility transmission system or off-grid. This process is crucial for the operation of PVS. Inverters can experience hardware failures and significant energy losses at PV sites [36]. Various types of inverter faults can lead to such issues. For example, manufacturing, design, and control problems, and electrical component failures are the major defects that can occur in inverters. These faults can cause a range of problems, from minor issues that can be easily fixed to major issues that can result in significant damage and downtime for the system [34].

To better understand the different types of inverter failures, Table II summarizes the various failure modes that can occur. Knowing these potential failures and addressing them promptly, PVS owners and operators can avoid unnecessary energy losses and ensure the proper functioning of their systems.

TABLE II
FAILURE MODES IN PV INVERTER COMPONENT

Element	Function	Cause of failure
IGBT	Convert DC to AC	Over-voltage, over-current, over-temperature, electrostatic discharge, latch-up and triggering of parasitics, charge effects of ionic contamination or hot carrier injection, external radiation [37].
Electrolytic capacitor	Stored energy	Over-voltage, harmonic current, high temperature, rapid charging, and discharging.
Fan	Inverter heat dissipation	The fan power supply is damaged, or foreign matters enter the fan.
MOSFET	Controlling current through field effects	Electrical stress, device structure or packaging issues [38].

C. Junction Box Faults

The solar junction box, a critical component in PVS, is a multifunctional device responsible for safeguarding solar modules, linking solar cells and external wiring, and directing generated solar cell power to external circuits. Various issues can afflict junction boxes, including poor fixation, wire corrosion, loose oxidation, and moisture penetration [34]. Such failures often precipitate physical harm and even fire incidents while degrading PVS's dependability and efficacy [18].

Over time, the junction box has entered the era of intelligence with the introduction of anti-shadow shielding intelligent junction boxes [39] designed to minimize the risk of failure. These innovations have ushered in a new era in PV technology, leveraging intelligence and ingenuity to surpass the constraints of traditional junction boxes. Compared to the traditional bypass diode junction box, the anti-shadow masking intelligent junction box achieves maximum power point tracking of a single PV panel through an improved particle swarm optimization (PSO) algorithm. This can effectively improve the output power of each PV module under shadow masking conditions during the PV module series connection process. It not only adapts to the complexity and variability of the PV module working environment, but also adjusts the PV module working voltage according to the load situation.

D. Bypass Diode Faults

Within a PV solar module, the bypass diode is a crucial component that helps prevent silicon cell burnout caused by the hot spot effect. This diode is connected in reverse parallel at both ends of the solar silicon cell pack in the battery module. One possible failure mode is a short circuit, which is relatively easier to detect than an open circuit. Unlike the latter, the former increases power loss in the module and does not immediately power down. The possible failure mechanisms can include electrostatic discharge, thermal fatigue, thermal runaway, etc. [40].

Thermal runaway occurs when the operating diode junction temperature exceeds the critical temperature during the transition from forward to reverse bias. Detecting bypass diode failure early is crucial for preventing potential hazards, such as decreased efficiency or even fires. So, it is necessary to thoroughly understand the bypass diodes and their failure modes to ensure the optimal performance of the modules [41].

E. Ground Faults

For PVS, GF can pose serious safety hazards and equipment damage. GF occurs when a current-carrying conductor unintentionally connects to a non-current-carrying conductor or ground, creating an abnormal flow of current that can cause fires, electric shocks, or equipment failure. While the potential causes of GF are diverse, some common culprits include cable insulation damage due to environmental factors such as aging, corrosion, or animal bites, internal GF inside PV modules, and short circuits caused by accidental contact between conductors and ground [11].

To diagnose GF in PVS, voltage-based methods have been widely used [42]. However, impedance-based approaches offer a more effective way of identifying GF. A healthy PVA has a specific impedance between pairs of nodes, while any GF will alter the impedance value, allowing for detection using spread-spectrum time domain reflection (SSTDR)-based methods [43]. PVS can be monitored through these techniques, and GF can be detected early, minimizing safety risks and preventing costly equipment failures.

F. Line-line Faults

Unexpected short circuit connection between two different potential points in a PVA may lead to LLF, such as short-circuit defects and double-ground faults [44]. Various methods are available for detecting LLF, each with advantages and limitations. For instance, the ensemble learning model based on *I-V* characteristics can effectively detect LLF by analyzing the voltage and current behaviors of the PV cells [45]. Similarly, the detection method based on current string behavior and current sensing can also provide valuable insights into the occurrence of LLF [46].

It is crucial to protect a PVA from LLF, and several protection standards are available to guide the process. However, these standards have different compatibility and shortcomings, and it is crucial to carefully assess and select the most appropriate measure for a given application. For example, the national electrical code (NEC), international electrotechnical commission (IEC), and underwriters laboratories (UL) protection standards can offer guidelines for LLF protection, but they also have their respective limitations [47].

G. Arc Faults

AF are a severe concern for grid safety and can result in fires. There are two main types of AF: series and parallel. Both types are hazardous and can cause severe damage to the grid. However, series AF poses a higher risk for fires than parallel because of its difficulty in detection [48]. This is because the current level decreases during series AF, so the over-current protection fuse will not activate.

In PVS, AF can also be classified as DC or AC. Unlike AC AF, DC AF in a PVS do not exhibit a zero crossing phenomenon, making it challenging to eliminate them. Also, the existing AC detection technologies are not directly applicable to DC detection [49].

AF detection methods are typically based on either current or voltage. For instance, the pseudo-Wigner-Ville distributed algorithm can be used for AF detection in PVS [50]. Unique detection methods can also be used, such as the series DC AF detection algorithm based on PV operating characteristics and detailed extraction of pink noise behavior [51].

IV. Fault Diagnosis Methods

There are many PV system fault diagnosis methods, based on different principles and methods. This section will mainly review and discuss the electrical methods for fault diagnosis of PVS. Conventional electrical methods can be divided into four categories:

1) Statistical and signal processing approaches (SSPA);
2) *I-V* characteristic analysis (IVCA);
3) Artificial intelligence technology (AIT).
4) Circuit structure method (CSM).

A. Statistical Signal and Processing Approaches

Analyzing waveform signals is the mainstay of SSPA. Time domain reflectometry (TDR), earth capacitance measurement (ECM), and SSTDR are three typical methods, and the three SSPA models are shown in Fig. 5. ECM is typically used to detect the disconnection position on transmission lines, which are considered as distributed parameter circuits. When a power transmission line experiences a disconnection fault, the ratio of the grounding capacitance value to the fault point (CX) and the capacitance value of the entire line (CD) is used to calculate the distance (X) from the starting point to the fault point, as shown in Fig. 5(a) [52]. The principle of the TDR diagnostic method is that when a signal is transmitted along a certain transmission path, any impedance change in the transmission path will be reflected by some of the signal while the other part of the signal will continue to transmit along the transmission path. TDR calculates the impedance change by measuring the voltage amplitude of the reflected wave. If the time from the reflection point to the signal output point is measured, the position of the impedance change point in the transmission path can be calculated. The SSTDR diagnostic method operates on the principle of generating a pseudo-random sequence using a signal generator. This sequence is then modulated by a local cosine to achieve spread spectrum characteristics. The modulated signal is subsequently transmitted as a test signal to the cable undergoing testing. When encountering a fault point, resulting in an impedance mismatch point in the cable, the test signal is reflected at that point and back to the sending end. The received signal is then correlated with the local reference signal for calculation. The delay of the two signals is determined through peak detection, and then the distance between the fault point and the signal sending end can be calculated [53].

The TDR and ECM fault diagnosis methods have been extensively discussed in literature [52]. Also, two methods for locating PV module string faults have been studied in outdoor experiments. It should be noted that ECM is particularly well-suited for detecting the disconnection position between modules in the series, irrespective of irradiance changes. TDR can be used in periodic inspections to detect system degradation. Reference [54] illustrates TDR's ability to detect, identify, and locate the most

common fault conditions, such as circuit interruptions, insulation defects, wiring abnormalities, etc.

Testing PVS with reflectometry is complex. With the recent addition of communication signals for fast shutdown, which can interfere with or be interfered by the TDR signal, an alternative to standard TDR is SSTDR. SSTDR has been proposed for ground fault diagnosis in PVS without relying on the amplitude of the fault current. Unlike TDR, which compares the signal from the input transmission line with the reflected signal caused by impedance mismatch in the bar, SSTDR is based on the impedance change in PVS caused by ground faults rather than the fault current value. It is highly immune to noise signals, making it a reliable option even without solar radiation [43]. Research in [55] shows that future arc faults can be predicted by measuring the impedance change without considering the inverter's working state.

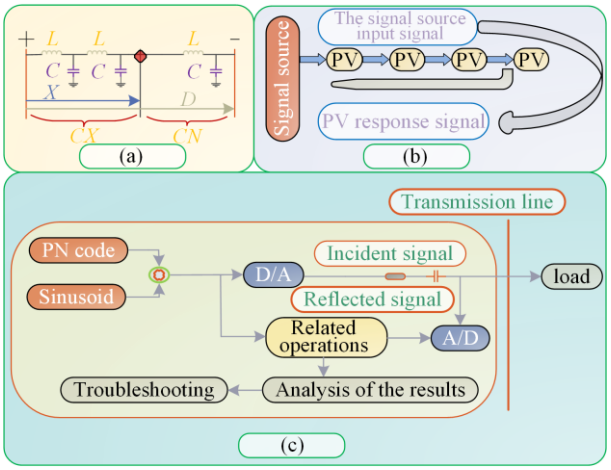

Fig. 5. Three SSPA models. (a) ECM model diagram. (b) Time domain reflectometry model. (c) SSTDR model diagram.

In [56], SSTDR can detect the natural aging or degradation state of the MOSFETs in a PV live inverter, allowing for the detection of any degradation related to the power semiconductor devices inside the circuit without interfering with the circuit's regular operation. Reference [57] proposes a fault location diagnosis method using SSTDR, where correlating the incident and reflected PN signals determines the distance to the fault. The study conducted in [58] delves into the employment of SSTDR to locate and detect disconnections in vast PV strings. The significance of SSTDR resolution, frequency, and attenuation in identifying disconnections within the system is analyzed. If these parameters are appropriate, disconnections within PVS can be judged, and the fault is detected and located by the peak of the signal. In [59], the ability of SSTDR to detect and locate damaged PV cells and modules in the string is evaluated. It is determined that bus damage can only be seen when an opening is created by cutting all inter-cell busbars.

Despite its succes, the study in [60] highlights the limitations of SSTDR in the fault diagnosis of several PVS. One such shortcoming is its susceptibility to environmental factors such as temperature and humidity. The precision of SSTDR-based fault diagnosis is greatly affected by the number of baselines. Consequently, a method for determining the number of baselines required for SSTDR-based fault detection under any climatic conditions is proposed.

B. I-V Characteristic Analysis

The IVCA method, based on the characteristic output curve law of PV modules, allows for the analysis and detection of faults based on voltage, current, and maximum power point indicators, which vary depending on the spot and environmental conditions. The *I-V* curve in a fault condition is shown in Fig. 6. While the traditional method of *I-V* curve acquisition is done through the use of handheld tools, advances in technology have given rise to alternative methods, such as the portable, lightweight method using capacitive load tracking PV string *I-V* curve [61] and the application of deep learning for automatic tracking.

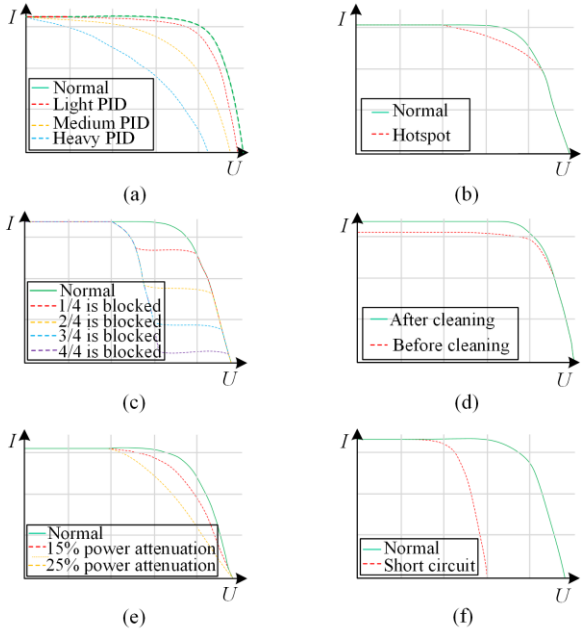

Fig. 6. *I-V* curve in a fault condition. (a) PID fault *I-V* curve characteristics. (b) Hotspot fault *I-V* curve characteristics. (c) Masking fault *I-V* curve characteristics. (d) Pollution fault *I-V* curve characteristics. (e) Aging fault *I-V* curve characteristics. (f) Bypass diode short circuit fault *I-V* curve characteristics.

Reference [62] investigates the relationship between *I-V* characteristics and various fault factors and the effect of irradiance and shadow coverage on *I-V* characteristics. Reference [63] introduces an efficient prediction model capable of predicting the *I-V* curve of PV modules at any irradiance and temperature value. This provides a means of addressing the uncertainty caused by environmental factors, as explored in [64]. This

proposes the use of a long short-term memory (LSTM) model for predicting the solar radiation and temperature of PV modules.

Reference [65] proposes to explore an online methodology for diagnosing cracks within PV modules using the *I-V* curve. The approach relies on the inconsistent reverse bias characteristics of pyrolysis PV modules, and the derivative method is employed to diagnose the crack fault of the PV module. [66] advocates a rapid diagnosis approach by comparing the *I-V* curve obtained from the component optimizer with the analyzed *I-V* curve for identifying HSF in PV modules. Reference [67] formulates an online diagnosis technique for a data-driven PV string current mismatch fault grounded on the *I-V* curve. This innovative approach can expediently and precisely detect the *I-V* curve's inflection point and step characteristics when the present mismatch fault occurs. Given that PID faults can be similar to other fault characteristics, most existing methods for diagnosing PID faults are costly and time-consuming.

In [68], the degree of the PID fault is assessed by detecting the open circuit voltage at high and low irradiation intensities. In [69], multiple fault diagnosis methods are integrated to create a step diagnosis method. The open circuit voltages of the component at high and low irradiances are obtained by *I-V* scanning, namely V_{oc1} and V_{oc2}, respectively. For $V_{oc1}/V_{oc2} \geqslant 1.1$, the component is deemed to have PID. Whenever there is no step, the aging threshold *FF* determines whether an aging failure occurs. When there is a step, the D_{max} value (the distance from the point on the *I-V* curve to the detection line) is employed to diagnose glass chipping and hot spot faults. A flowchart is illustrated in Fig. 7 to elucidate this process further.

In [70], a novel technique for estimating PV module degradation is proposed that involves the extraction of the *I-V* curve under specific conditions, i.e., before the inverter is activated, thus avoiding the need for any additional circuitry or data and allowing for uninterrupted operation. [71] empirically demonstrates that the d*I*/d*V*-*V* curve. Reference can be used to diagnose the degradation of the PVS. The variance value of an abnormal PV subarray differs greatly from that of a normal one, regardless of the influence of weather factors. Reference [72] combines a hybrid artificial bee colony and a semi-supervised extreme learning machine (ABC-SSELM) while also considering the impact of dust. The ABC-SSELM diagnostic model requires only a small amount of labeled data and has high accuracy.

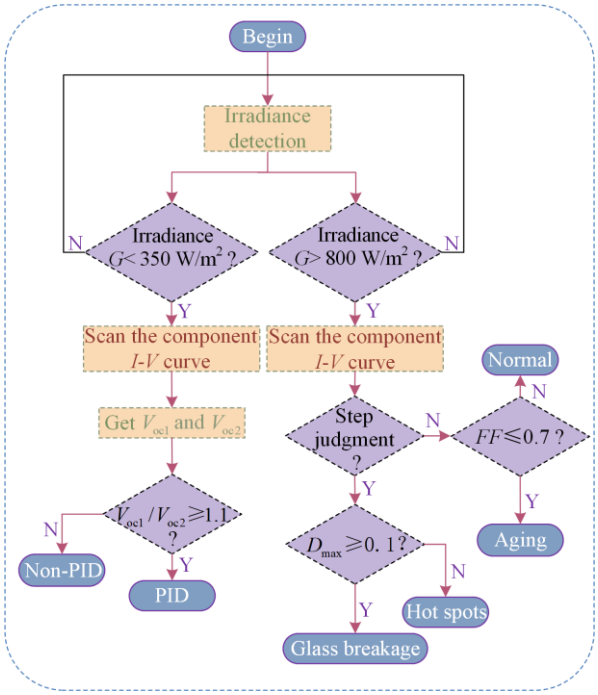

Fig. 7. IVCA step method flow chart.

C. Artificial Intelligence Techniques

Although electrical methods are widely used, artificial intelligence diagnostic methods are constantly being developed. They are divided into three categories:

1) Neural network methods (NNM);

2) Support vector machine (SVM) methods;

3) Fuzzy control algorithm methods (FCAM).

In order to better understand the advantages and differences of different types of AIT diagnostic methods, Table III summarizes various AIT diagnostic methods.

Table III
AIT DIAGNOSTIC METHOD STATISTICS

Diagnostic methods	Method subclass	Optimize the direction
NNM	BP neural networks [79], [80]	The learning process converges quickly and robustly.
	RBF neural networks [81]	Reduce environmental impact.
	PNN neural networks [82]	Reduce the sample size.
	LSTM neural networks [83]	Add fault identification methods.
	ART neural networks [84]	It enhanced signal extraction capabilities.
	BAM neural networks [85]	Remove redundant failure data.
SVM	KNN-SVM [87]	Increase classification rates.
	Genetic algorithm VCM [90]	Core parameters are optimized.
	PSO-VCM [91]	Core parameters are optimized.
	ABC-SVM [92]	Core parameters are optimized.
	SOA-SVM [93]	Core parameters are optimized.
FCM	FM-FCM [96]	Calculates the degree of membership of the running data to the cluster center.
	SRF-FCM [97]	Create a new classification model.
	3σ-FCM [98]	Only fault string current is required.
	GKFCM [100]	Eliminate the problem of noise and failure that is difficult to distinguish.

1) Neural Network Method

Fault diagnosis is a challenge in PVS. Various NNM have been developed to tackle this issue, each with unique neural network structures. The core of artificial intelligence network fault diagnosis methods is to determine the number of nodes and layers, and first requires fault feature selection and processing of the original data. There are many methods for feature extraction, such as using fault tree analysis to obtain the minimum cut set of the fault tree by replacing the bottom event matrix with logic gates [73], and then using wavelet features to obtain representative high-frequency signals, along with string current and open circuit voltage, as inputs to the neural network [74]. Some methods use PVA output voltage, output current, output power, inverter output voltage, output current, and light intensity as inputs [75]. The most widely used feature quantities are the maximum power point voltage (U_{mmp}), maximum power point current (I_{mmp}), open circuit voltage (U_{oc}), and short circuit current (I_{sc}) [76]. In addition, a method to reduce the number of nodes and layers by denoising the original data is used. Because of external influences, the data contains noise, so the denoised data leads to better training effect [77].

One of the most widely used NNM is the back propagation (BP) neural network, first introduced in 1986 by Rumelhart and McClelland. This machine learning algorithm is particularly suited for dealing with nonlinear problems, which they often are in PVS fault diagnosis. The BP neural network consists of a three-layer network, namely the input, output and hidden layers. The input variables for the input layer of the BP neural network model proposed in [76] are U_{mmp}, I_{mmp}, U_{oc}, and I_{sc} of the PVA. The corresponding output variables can reflect PVS faults in four different situations: short circuit, open circuit, abnormal aging, and local shadows. The BP neural network structure diagram is shown in Fig. 8.

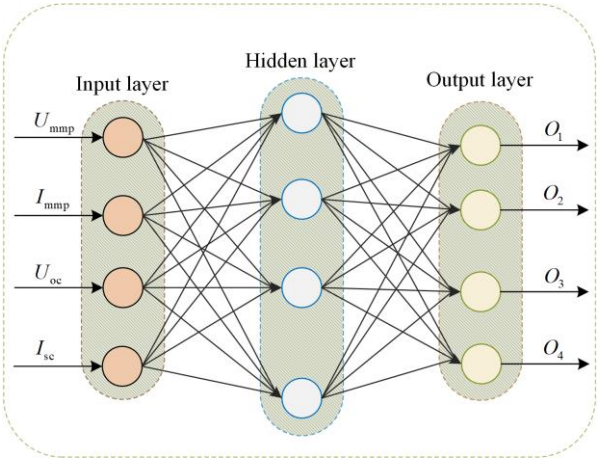

Fig. 8. BP neural network structure diagram.

The number of nodes in the hidden layer is a crucial issue, and can be determined by either of the following two formulas:

$$n_1 = (n+r)^{\frac{1}{2}} + a \tag{1}$$

where n_1 is the number of hidden layer elements; n is the number of input units; r is the number of output units; and a is a constant between 1 and 10.

$$n_1 = \log_2 n \tag{2}$$

Since the four-parameter units of the input layer are different, and their order of magnitude difference is large, it is necessary to normalize the input layer data by [78]:

$$P_n = \frac{I_n - I_{\min}}{I_{\max} - I_{\min}} \tag{3}$$

where I_n is the original input data; $I_{\max}$ and $I_{\min}$ are the maximum and minimum values in the original input data; and P_n is the normalized input data. The ANN diagnostic flowchart is shown in Fig. 9.

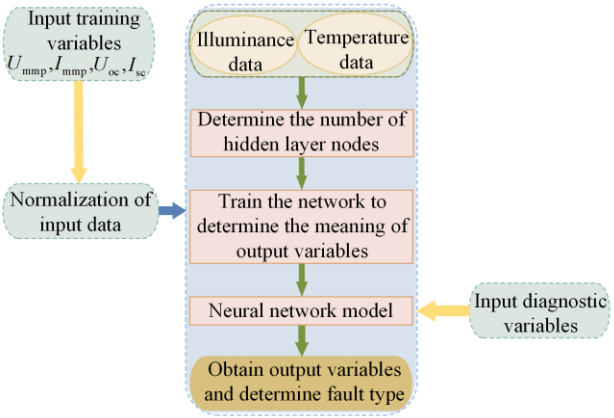

Fig. 9. ANN diagnostic flowchart.

In recent years, other neural network algorithms have also been proposed with unique advantages. For instance, reference [79] offers a PVA fault diagnosis method using a BP neural network optimized by a genetic algorithm, which optimizes the weight and threshold of the BP neural network by using the genetic algorithm's global search performance to improve convergence speed and accuracy. Similarly, reference [80] proposes a PVA fault diagnosis method based on adaptive weighted particle swarm optimization (AWPSO) for a BP neural network. This can solve the problems of slow convergence, poor robustness, and quickly falling into a local minimum. It does this by exploiting AWPSO's good global search capability. Additionally, reference [81] proposes a fault-diagnosis method for PV modules with an improved radial basis function (RBF) neural network based on a k-means clustering algorithm. This achieves a fault diagnosis accuracy rate of 96.67%.

Reference [82] investigates a PVA fault diagnosis method based on a probabilistic neural network (PNN).

The PNN is a relatively simple feed-forward neural network proposed in 1989 that can replace nonlinear learning algorithms with linear learning. PNN consists of the input, pattern (hidden layer), summation layer, and decision layers (output layer). The input variables are also typically U_{mmp}, I_{mmp}, U_{oc} and I_{sc}. A PVA fault diagnosis model based on an LSTM neural network is proposed in [83], which studies the influence of different fault states on the output characteristics of PVS through simulation and then obtains fault characteristic parameters. Reference [84] develops a PV fault diagnosis method based on an improved adaptive resonance theory (ART) neural network, which characterizes different fault characteristics using a matrix, allowing for the accurate diagnosis of PVS faults. In addition, reference [85] investigates a fault diagnosis method that integrates the theory of the fault tree (FT) and bidirectional associative memory (BAM) neural network.

2) Support Vector Machine Method

In machine learning, SVM is a classic binary classification algorithm with low sample demand, short training time, good classification recognition effect, and strong generalizability. The core concept of SVM is to construct an optimal hyperplane that classifies distinct data points and maximizes the classification interval. The principle is illustrated in Fig. 10, where H denotes the hyperplane, while H_1 and H_2 are the parallel classified surfaces that are equidistant from H. The optimal hyperplane H can be obtained by maximizing the spacing between H_1 and H_2. For a linearly separable training sample data set (x_i, y_i), $i=1,2,\cdots,n$, $x_i \in R_d$, $y_i \in \{1,-1\}$, the categorical hyperplane equation is expressed as $wx+b=0$. The optimal hyperplane can be determined by transforming it into a constraint-based formulation and solving the subsequent equation of:

$$\begin{cases} \phi(w,\zeta)=\dfrac{1}{2}\|\boldsymbol{w}\|^2+C\sum\limits_{i=1}^{n}\zeta_i \\ \text{s.t. } y_i(\boldsymbol{w}^{\mathrm{T}}x_i+b)+\zeta \geqslant 1 \end{cases},\ i=1,\cdots,n \tag{4}$$

where $\boldsymbol{w}$ is the weight vector of the hyperplane; b is the bias; ξ is the relaxation variable; C is the penalty factor that determines the magnitude of ξ; and s.t. represents the constraint condition.

To solve the optimization problem, the Lagrange dual function is constructed as:

$$\begin{cases} \max L(\alpha)=-\dfrac{1}{2}\sum\limits_{i=1}^{n}\sum\limits_{j=1}^{n}\alpha_i\alpha_j y_i y_j (x_i,x_j) \\ \text{s.t. } \sum\limits_{i=1}^{n}\alpha_i y_i=0, \quad 0\leqslant\alpha_i\leqslant C \end{cases} \tag{5}$$

where α is the Lagrange multiplier. When mapping low-dimensional data to high dimensions, the kernel function needs to be determined, max represents the maximum value.

The optimal classification function is given by:

$$f(x)=\text{sgn}[\sum_{i=0}^{n}\alpha_i y_i K(x_i,x_j)+\hat{b}] \tag{6}$$

where $K(x_i,x_j)$ is the kernel function; sgn is a step function; and $\hat{b}$ is the estimated value of b. The selection of different kernel functions impacts SVM's classification ability and application scope. Commonly used kernel functions include the polynomial, linear, Gaussian, and sigmoid kernel functions. The SVM diagnostic flowchart is shown in Fig. 11.

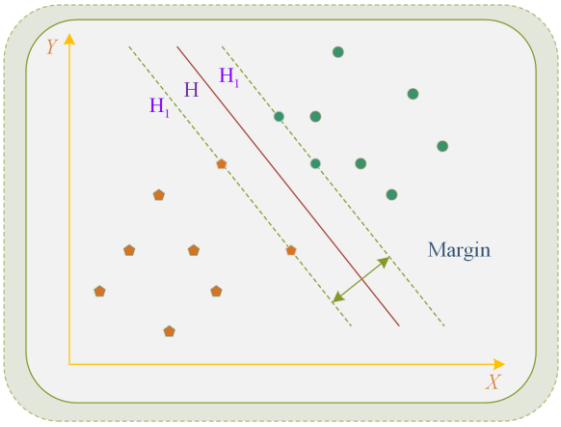

Fig. 10. Schematic diagram of SVM.

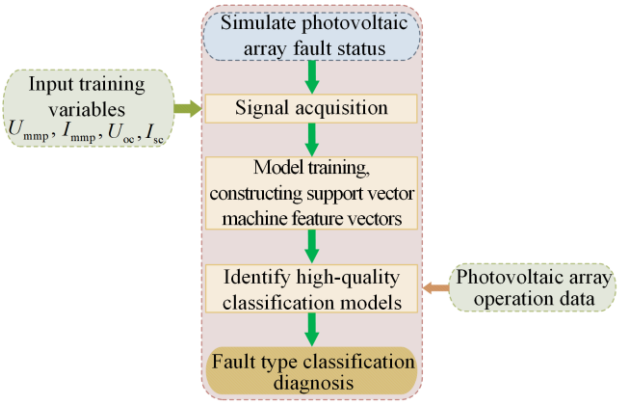

Fig. 11. SVM diagnostic flowchart.

In the realm of DC PVS, researchers have proposed various AF detection and diagnosis methods. An approach based on wavelet transform and SVM is introduced in [86], where features are extracted from the voltage/current signals using wavelet transform. SVM is used for AF identification, e.g., reference [87] presents an intelligent algorithm for PV generator short circuit detection and diagnosis using a hybrid classifier produced by a mixture of SVM technology optimized by the K-NN tool. The proposed hybrid classifier exhibits high classification and low error rates.

Reference [88] proposes an AF detection method based on Hilbert spectral analysis, singular value de-

composition, and SVM, effectively overcoming the influence of different loads and noise on feature extraction. Reference [89] reports an accuracy rate of 99.4% for fault detection and 98% for fault diagnosis, while the technology employed does not require any AC variable of PVS. In [90], genetic algorithms are proposed to optimize the PVA fault diagnosis of SVM. The parameters are optimized using a genetic algorithm, resulting in a significant improvement in classification accuracy. In [91], the particle swarm optimization (PSO) algorithm is used to optimize the parameters, and the PSO-SVM PVA fault diagnosis model is established. The fault detection accuracy of the model reaches 99.89%, and the classification accuracy is 98.68%. Reference [92] uses an artificial bee colony algorithm to optimize the fault diagnosis mode of SVM, achieving higher diagnostic accuracy than the PSO-SVM model, whereas reference [93] demonstrates that the fault diagnosis accuracy of the SVM model after seagull optimization algorithm (SOA) optimization is significantly improved.

3) Fuzzy Control Algorithm Methods

FCAM are generally based on the fuzzy C-means (FCM) clustering algorithm for fault diagnosis. The FCM clustering algorithm uses the membership function to establish the degree to which each data point belongs to a particular cluster. The algorithm automatically classifies the sample data by obtaining the membership degree of each sample point to all class centers by optimizing the objective function. The FCM algorithm flowchart is shown in Fig. 12.

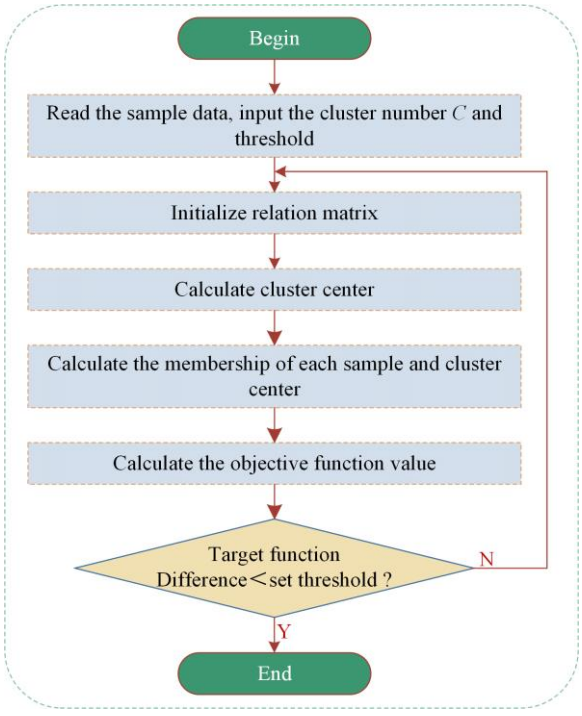

Fig. 12. FCM algorithm flowchart.

To achieve this, FCM clustering divides the poly scale $x_j (j=1,2,\cdots,n)$ corresponding to n PV power generation units into c subgroups, and finds the center point v_i $(i=1,2,\cdots,c)$ of the clustering index in each group so that the objective function value reaches the minimum. The objective function is a marvel of complexity, shown as:

$$J_m = \sum_{i=1}^{c}\sum_{j=1}^{n} \mu_{ij}^{m} \left\| v_i - x_i \right\|_2 \tag{7}$$

where $\left\| v_i - x_i \right\|_2$ is the Euro-style distance between the ith cluster center point and the jth PV power generation unit clustering index; $m \in [1,\infty)$ is the fuzzy coefficient, generally taken as 2; and μ_{ij} is the membership degree value of the group corresponding to the ith cluster center point of the jth PV power generation unit. It meets the normalization requirements:

$$\text{s.t.}\begin{cases} \sum_{i=0}^{c} \mu_{ij} = 1, \quad 1 \leqslant j \leqslant n \\ \mu_{ij} \in [0,1], \quad 1 \leqslant j \leqslant n, \quad 1 \leqslant i \leqslant c \\ n > \sum_{j=0}^{n} \mu_{ij} > 0, \quad 1 \leqslant i \leqslant c \end{cases} \tag{8}$$

To find the necessary conditions for the minimum value of (8), a function is constructed:

$$\bar{J}_m = J_m + \sum_{j=1}^{c} \lambda_i \left(\sum_{i=1}^{c} \mu_{ij} - 1 \right) \tag{9}$$

where λ_i is the Lagrange multiplier of the n constraints of (9). Finally, to derive all input parameters, the necessary conditions for (8) to reach the minimum value are expressed by the following equation:

$$\begin{cases} v_i = \dfrac{\sum_{j=1}^{n} \mu_{ij}^{m} x_j}{\sum_{j=1}^{n} \mu_{ij}^{m}} \\ \mu_{ij} = \dfrac{1}{\sum_{k=1}^{c} \left(\dfrac{\left\| x_j - v_j \right\|_2}{\left\| x_j - v_k \right\|_2} \right)^{\frac{2}{m-1}}} \end{cases} \tag{10}$$

The FCM algorithm output comprises two fundamental parts. The first part features c clustering center points, each representing the average characteristics of the corresponding group's PV power generation unit clustering index. The second part has a fuzzy division matrix of ($c \times n$), indicating the membership degree of each PV power generation unit belonging to each group. The group to which each unit belongs is determined according to the fuzzy set maximum membership principle [94].

Reference [95] uses an algorithm combining FCM and normal distribution membership functions. This method sorts the membership sizes to get the type of failure of the diagnosed sample. In [96], the fuzzy membership (FM) algorithm is leveraged to calculate

the membership degree of operating data and clustering centers, thus determining typical fault types of the PVA. However, when the PVA to be diagnosed is too large, diagnosing subtle faults can become challenging. To address the issue, reference [97] proposes a PV fault diagnosis method that combines the algorithm based on the stacking random forest (SRF) method with FCM. This method uses the FCM-SRF classification model composed of the clustering center and SRF classification model obtained by FCM to judge the status of PV modules. In [98], the three times standard deviation (3σ) criterion and FCM algorithm is combined, and the difference between PV strings, combined with the 3σ bar, is used to obtain the string fault factor. This helps to locate the DC side fault of the PV power station with the use of current string data only.

Reference [99] explores the diagnosis of the health state of the PVS. This is divided into four categories: health, sub-health, partial shadow, and fault state. The cluster center is obtained through FCM, while the paper also summarizes three indicators that affect the health status of PV modules, namely, light transmittance, series and parallel resistances. Reference [100] proposes a fault diagnosis method for PVA based on Gaussian FCM (GKFCM), which eliminates the difficulty of distinguishing between multiple faults and a single fault, and the problem of data noise by normalizing the three characteristic quantities of voltage V_{norm}, normalized current I_{norm}, and fill factor *FF*.

D. Circuit Structure Method.

The PVS is a complex network of multiple PV modules in various configurations, including series and parallel connections. To diagnose faults in such systems, CSM involves adding sensors to the circuit to detect the current or voltage of each module. The data collected in the fault state are then compared with the standard data to determine whether there is a fault. However, this method has its limitations, particularly when applied to large-scale PV power plants requiring many sensors. Adding such sensors can be prohibitive, and the amount of analysis data needed can be overwhelming [101].

To address these issues, researchers have been exploring ways to improve the circuit structure of the PVS. One such approach is the series-parallel (SP) array, introduced in [102]. This array comprises *N* strings and *M* components. Its fault diagnosis involves identifying the faulty string through the current sensor, determining the wrong branch, and then diagnosing the fault PV module using the voltage sensor. The schematic diagram of the SP structure is shown in Fig. 13(a).

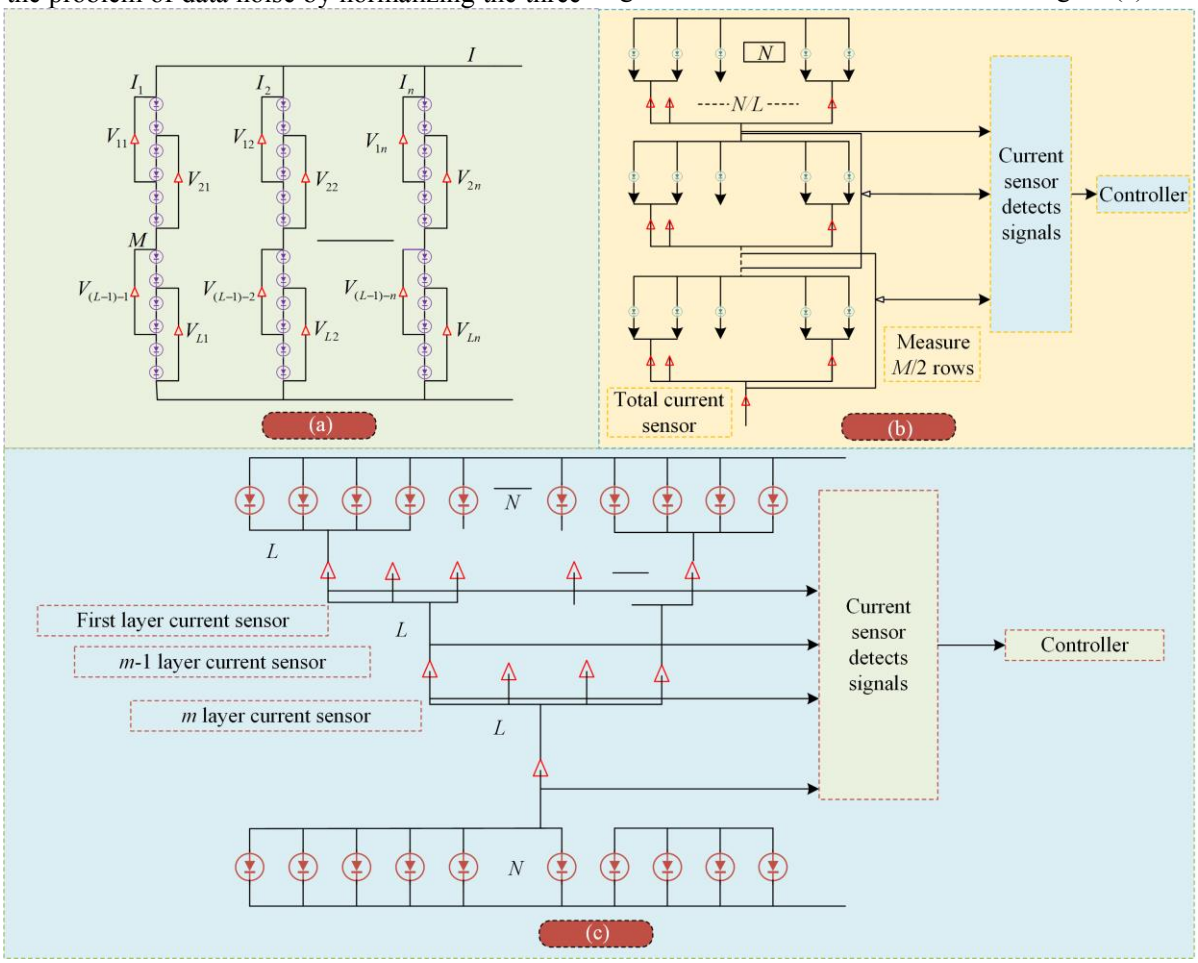

Fig. 13. Three types of circuit structure diagrams. (a) SP structure schematic. (b) TCT structure schematic. (c) CTCT structure schematic.

Reference [103] proposes a circuit structure method for the total-cross-tied (TCT). When the circuit structure of a PV array adopts a TCT structure, *N* PV modules are first connected in parallel and then connected in series. A PVA using this structure mainly uses current sensors to diagnose PV module faults. Compared with the fault diagnosis method for PV modules based on SP structure, the fault diagnosis method for PV modules based on TCT structure significantly reduces the number of current sensors and detection costs. It measures the total output current and total voltage of the PV array during normal operation. The faulty row position is determined based on the values of each voltage sensor, and then the faulty column position is determined based on the values of the current sensors connected to each row of the parallel PV cells. If the current value measured by a current sensor is less than the average of the total current, the fault is located in the column of the current sensor with the lower measured current value. The TCT structure schematic is shown in Fig. 13(b).

Another circuit structure proposed in [104] is based on the complex-total-cross-tied (CTCT) array method. The fault diagnosis of CTCT structured PVA is to equate the PV cells of a TCT structured PVA to a connection method of first parallel and then series connection. Each layer is composed of *N* PV cells in parallel, and two adjacent layers are connected to the current sensors of layer *m*. The current values of the current sensors in layer m are compared with the set value to determine the location of the fault, and then the current values of the current sensors in layer *m*-1 are sequentially detected until the first layer. The CTCT structure schematic is shown in Fig. 13(c).

In summary, while the conventional CSM method for fault diagnosis in a PVS has its limitations, new and innovative ways are being developed to improve the circuit structure of the systems to reduce the number of sensors required while maintaining accurate fault diagnosis.

E. Other Fault Diagnosis Techniques

Currently, most PV fault diagnosis methods are electrical diagnosis methods, whereas some nonelectrical diagnosis methods have also been proposed. This paper provides an overview of nonelectrical diagnosis methods which are divided into two categories:

1) Infrared image analysis (IIAM);
2) Mathematical model (MMM).

1) Infrared Image Analysis Method

IIAM is a diagnostic approach based on the fundamental principle of dividing infrared rays into near-, mid- and far-infrared rays based on their different wavelengths. Objects usually have different temperatures, and higher temperature objects emit more radiation than low temperature objects. The general infrared image analysis method collects the radiation intensity of the object through the thermal imager, and then it processes and analyzes the image to carry out fault diagnosis. IIAM has been categorized into three stages: data collection, feature extraction, and classification.

Reference [105] proposes a method to diagnose whether the PV module has a hot spot fault according to the Matlab algorithm and locate where the hot spot fault occurs. The method is shown in Fig. 14, and it has the advantage of high accuracy and can diagnose the location and number of defects. A non-contact electromagnetic induction excitation infrared thermal imaging technology is proposed in [106]. The general infrared thermal imaging technology is passive and can only carry out large-scale fault diagnosis and rough detection.

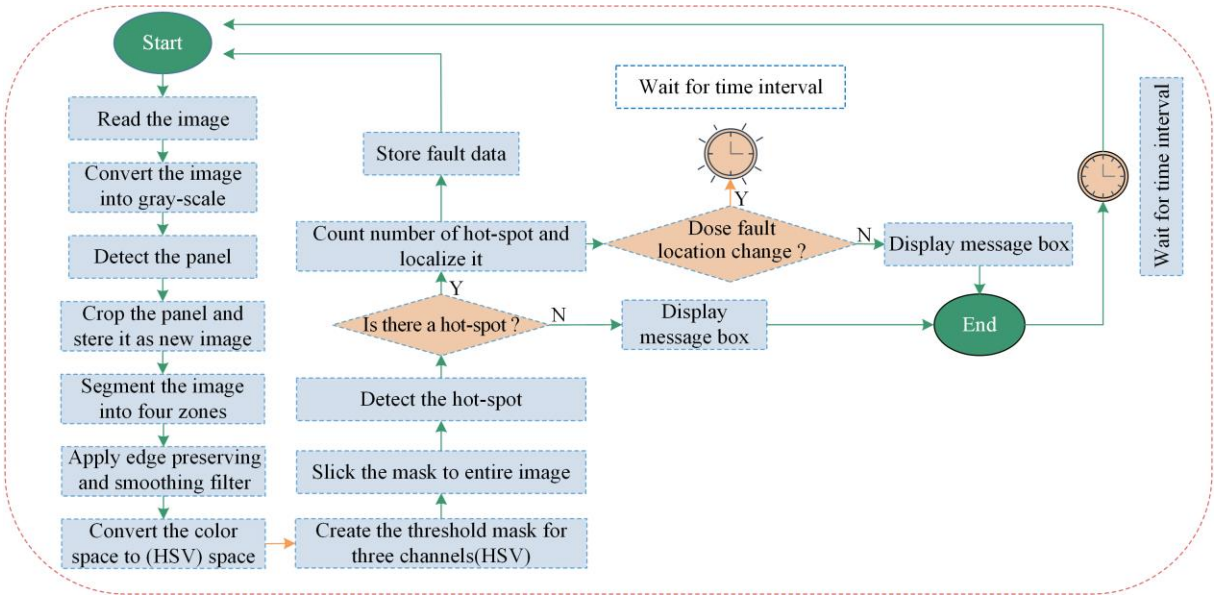

Fig. 14. Infrared flow chart.

However, with the emergence of various PV cells, the internal structure of PV cells is more complex, and the forms of damage are passive, so thermal imaging can only detect faults in the power generation state. The method proposed is an active electromagnetic, infrared imaging technology, also known as eddy current thermal imaging. This method uses electromagnetic induction (EMI) parameters to provide a heating effect with EMI, generating eddy currents and temperature fields. Defects such as cracks and damages affect eddy currents and thermal diffusion, resulting in abnormal surface temperature of PV cells and modules. Thus, it is more effective to distinguish defects in PV cells and modules when the temperature of PV modules rises rapidly.

2) Mathematical Model Method

The essence of MMM is to create an equivalent model which is then simulated through various software such as Matlab, Pspice, Psim, etc. while keeping a tab on different environmental factors and other influencing factors. A predictive mathematical model is established by collecting corresponding data, which are then compared with the mathematical model obtained from the field data to diagnose the PV failures. The flow chart of the mathematical model method is shown in Fig. 15.

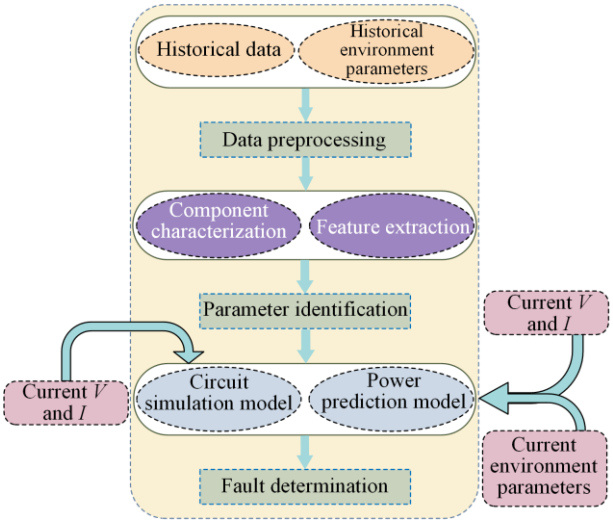

Fig. 15. Flow chart of mathematical model method.

The PV equivalent circuit diagram in Fig. 16 is usually followed to construct the mathematical model. Then a series of formulas are derived through Kirchhoff's current and voltage laws to establish the corresponding mathematical model. In Fig. 16, I_{ph} represents the photogenerated current of the PV module; R_L represents an equivalent external load of the PV module; while R_S and R_{sh} represent the equivalent series and parallel resistances of the PV module, respectively; the voltage at the output of PV module is represented by V; and the current at the output of PV module is represented by I [107]. The relationship between the parameters in Fig. 16 can be expressed as:

$$I = I_{ph} - I_0[\exp(\frac{q(V+IR_S)}{d\sigma T} - 1)] - \frac{V+IR_S}{R_{sh}} \quad (11)$$

where I_0 is the reverse saturation current of the diode; d is the ideal factor of the diode; σ is the Boltzmann constant (1.38×10^{-23} J/K); q is the electron charge and the value is 1.602×10^{-19} C.

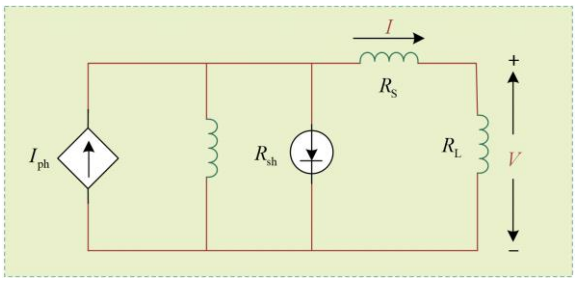

Fig. 16. Equivalent circuit diagram of a PV module.

Reference [108] proposes an equal division method that uses an iterative data method to obtain the PV *I-V* characteristics of the mathematical model. The *I-V* feature is used to obtain the minimum value of R_{sh}, while R_{sh} can be derived from (11). If its minimum value is too small, the current value will also decrease accordingly, causing excessive deviation of the *I-V* curve. Reference [109] proposes a unidirectional diode-based model, which uses an iterative method to determine all diode key parameters, whereas [110] offers a way to determine the five parameters of PV modules without the iterative process. Reference [111] suggests a concept of the influence of weather factors on the performance of PV devices, and applies the structure identification method of interval difference equation to form an interval discrete model. To more clearly demonstrate the performance and applicability of various FD methods, Table IV summarizes the various fault technologies of PVS.

TABLE IV
FAULTS DIAGNOSIS METHODS IN PVS

Methods		Reference	Year	Subjects	Temporally or permanent	Online or offline	Complexity / integration	Economic	Accuracy
SSPA	TDR and ECM	[54]	1994	Detect, identify, and locate the most common fault conditions, such as circuit interruption, insulation defect, wiring abnormality, etc.	Permanent and temporally	Online	***	***	***

Continued

Methods	Reference	Year	Subjects	Temporally or permanent	Online or offline	Complexity / integration	Economic	Accuracy
	[52]	2007	Locate the PV module string fault, detect the disconnection position between modules in the string, and detect the degraded position (see the increase of series resistance between modules).	Permanent	Online	**	***	**
SSTDR	[43]	2013	Grounding fault diagnosis of PVS.	Permanent	Online	***	*****	****
	[55]	2014	Arc fault diagnosis of PVS.	Permanent	Online	****	*****	****
	[56]	2014	Determine the internal impedance of the PV inverter, and detect the natural aging or degradation state of MOSFETs in the PV live inverter.	Permanent	Online	***	***	***
	[57]	2018	Diagnose the fault location of PVS.	Permanent	Offline	*****	****	***
	[59]	2020	Detection of bus damage and physical impact damage to glass and silicon of full-size PV modules.	Permanent	Offline	****	***	**
	[58]	2021	Detect and locate disconnection in large-scale PV strings.	Permanent	Online	***	***	**
	[60]	2021	PVS fault diagnosis.	Permanent	Offline	***	***	**
IVCA	[71]	2002	Diagnosis of PVS degradation.	Permanent	Online	***	***	***
	[62]	2003	Diagnose the failure of PVS and judge the loss factors (such as shadow degradation, disconnection, and other factors).	Both	Online	***	***	**
	[66]	2019	Rapid diagnosis of PV module hot spot failure.	Permanent	Online	***	***	***
	[69]	2019	Diagnosis of PVS PID, aging, glass crack, hot spot.	Both	Online	****	***	***
	[65]	2020	Effectively diagnose PV module cracks and local shadow faults.	Permanent	Online	***	***	****
	[68]	2021	Diagnose PVS PID fault.	Permanent	Online	***	*****	****
	[70]	2021	Estimate the degradation of PV modules.	Permanent	Online	***	***	***
	[67]	2022	On-line diagnosis of PV string current mismatch fault.	Permanent	Online	****	*****	***
	[72]	2023	It can effectively identify faults under short circuits, two types of partial shading, abnormal aging, dangerous pollution, and pollution conditions.	Both	Online	****	***	***
AIT NNM	[85]	2013	It can diagnose PVA failure, battery failure, transformer failure, relay failure, AC power failure, primary circuit failure, etc.	Permanent	Offline	***	*****	**
	[79]	2021	Diagnose open circuit faults, short circuit faults, aging faults, and shadows to improve its diagnostic accuracy.	Both	Online	***	***	****
	[80]	2021	Diagnose open circuit faults, short circuit faults, aging faults, and local shadow faults to improve timeliness.	Both	Online	***	***	****
	[81]	2021	To uneven light, detailed simulation analysis of electric breakdown and thermal breakdown, open circuit fault, and short circuit fault caused by lighting.	Permanent	Online	**	*****	***
	[82]	2021	Diagnose open circuit faults, short circuit faults, aging faults, and local shadows.	Both	Online	***	***	**
	[83]	2021	Accurately identify and locate faults such as open circuit, partial occlusion, shadow occlusion, and ash accumulation of PVA, and pre-judge PV hot spot faults in advance.	Both	Online	**	***	***
	[84]	2022	Accurately identify short circuits, open circuits, shadow shielding, aging, and other faults.	Both	Online	***	*****	***
SVM	[87]	2014	PV generator short circuit detection and diagnosis.	Permanent	Online	***	***	***
	[86]	2016	Arc fault diagnosis of DC PVS.	Permanent	Online	****	***	**
	[91]	2017	Diagnosis and classification of open circuits, short circuits, and shadow faults of PV modules.	Both	Online	***	***	**
	[89]	2019	Distinguish between free fault, permanent fault (line, open circuit), and temporary fault (partial shadow) in the PVA.	Both	Online	***	***	**
	[90]	2019	Diagnose the short circuit, open circuit, aging, and blocking fault of one or more components.	Permanent	Online	****	***	***
	[88]	2021	Arc fault diagnosis of PVS.	Permanent	Online	***	***	***

Continued

Methods		Reference	Year	Subjects	Temporally or permanent	Online or offline	Complexity / integration	Economic	Accuracy
		[92]	2021	Diagnosis and classification of open circuits, short circuits, and shadow faults of PV modules.	Both	Online	***	*****	****
		[93]	2022	Diagnosis and classification of open circuits, short circuits, and shadow faults of PV modules.	Both	Online	***	*****	*****
	FCAM	[95]	2016	Diagnosis and classification of open circuits, short circuits, shadow faults, and multiple mixed faults of PV module.	Both	Online	***	***	***
		[96]	2018	Determine the short circuit, open circuit, partial shielding, and other faults of PV modules.	Both	Online	****	*****	***
		[98]	2018	DC side fault location.	Permanent	Online	****	***	****
		[100]	2018	Diagnose short circuits and open circuit faults of PV modules.	Permanent	Online	***	***	***
		[97]	2019	Diagnose the internal short circuit, global shadow, local shadow, abnormal aging, and other faults of PV modules.	Both	Online	****	*****	***
CSM	CTCT	[104]	2010	PVS hot spot fault diagnosis.	Permanent	Offline	**	*****	*****
	SP	[102]	2017	Diagnosis of open circuit faults in PVS.	Permanent	Offline	**	*****	***
	TCT	[103]	2019	Diagnosis of open circuit faults in PVS.	Permanent	Offline	**	*****	***
IIAM	Other fault diagnosis techniques	[106]	2018	Diagnose defects such as hot spot microcracks, broken grids, surface impurities, etc., of PV cells and modules.	Permanent	Online	****	***	**
		[105]	2022	Diagnose and locate the hot spot fault inside the PV module.	Permanent	Online	***	***	***

V. CONCLUSIONS

This paper delves into the perplexing and intricate topic of PVS fault diagnosis. We classify and summarize the diverse diagnostic methods of PVS. They can be broadly categorized into SSPA, IVCA, AIT, CSM and other methods. Comparison and evaluation of the five types of FD methods are shown in Fig. 17, and the diagnostic methods applicable to various fault types are also summarized in Table V. To provide a comprehensive and insightful understanding of these methods, this paper systematically introduces and analyzes the different technologies in detail. The main conclusions are summarized as follows:

TABLE V
SUMMARY TABLE OF DIAGNOSTIC METHODS FOR VARIOUS FAULT TYPES.

Type of faults		Failure diagnosie method									
		SSAPA			IVCA	AIT			CSM	Other fault diagnosis techniques	
		ECM	TDR	SSTDR		NNM	SVM	FCAM		IIAM	MMM
PV module failures modes	EVA discoloration				√	√					
	Delamination				√					√	
	HS				√			√	√	√	√
	PID				√						
	LID				√						
	Shading and soiling				√	√	√	√	√		√
Inverter failure modes				√		√					
Bypass diode failures					√						
Junction box failures								√			
Ground faults		√	√	√		√					
Line-line faults			√		√		√				
Arc faults				√			√	√			

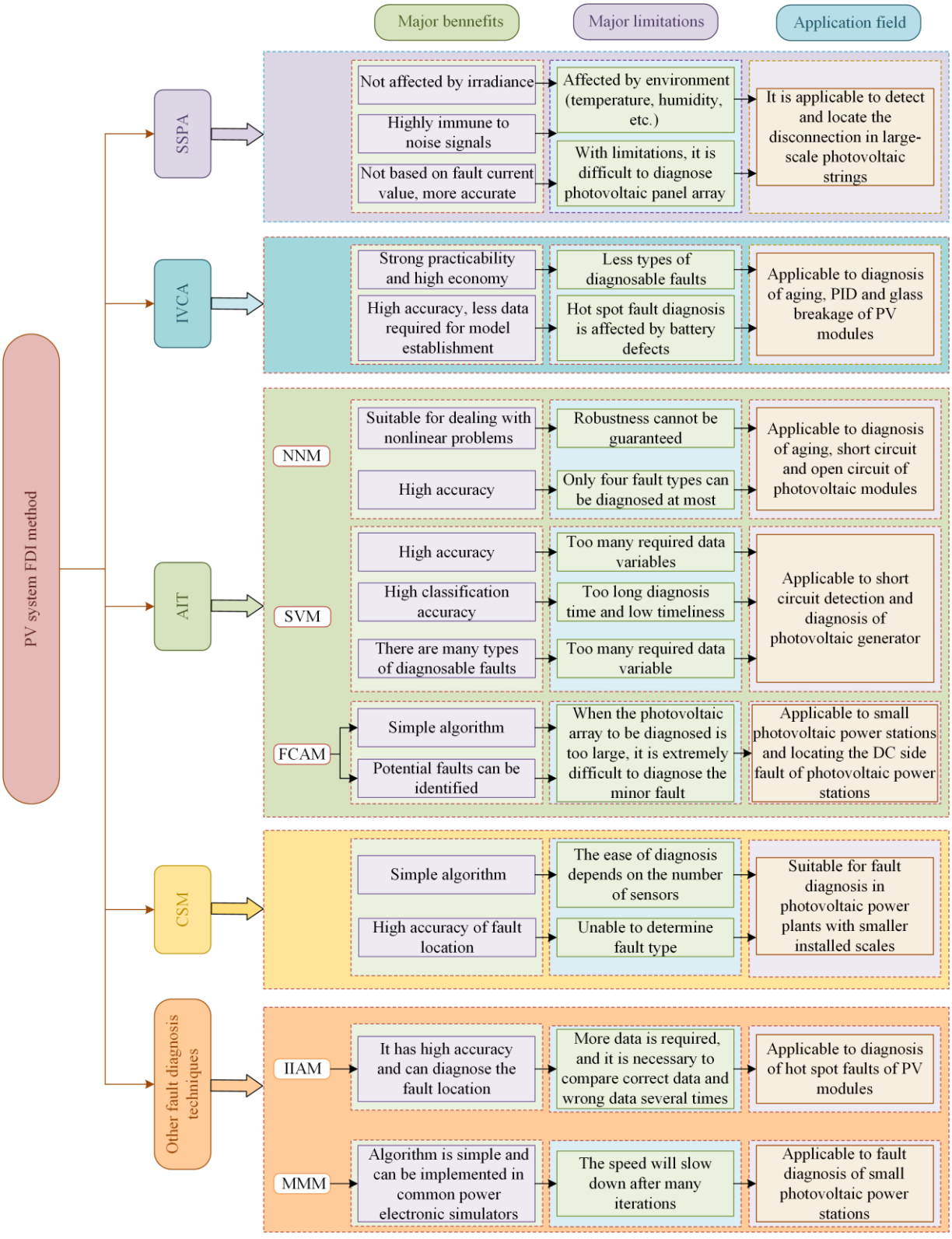

Fig. 17. Comparison and evaluation of four types of FD methods.

1) The SSPA diagnostic methods in PVS fault diagnosis can be divided into TDR, ECM, and SSTDR. SSTDR is more extensively applied than TDR since it is not susceptible to signal interference. TDR is primarily used to diagnose component degradation, whereas ECM and SSTDR mainly diagnose PV module disconnection faults.

2) The IVCA method is predominantly used to diagnose PID, HSF, and aging faults. This approach's primary advantage is its low cost, as it only requires obtaining *I-V*

curves for diagnosis without additional expensive machines. However, the accuracy of this method is dependent on the analysis algorithm employed.

3) The AIT methods comprise NNM, SVM, and FCAM. NNM relies on the neural network model to improve diagnostic accuracy, while using various algorithms to optimize the network model. SVM is optimized through multiple algorithms to ensure the obtained PVS model data is more accurate, and FCAM also optimizes the model through algorithms. The common advantage of these three methods is their high accuracy.

4) CSM mainly uses SP, TCT, and CTCT circuit connection methods. The implementation process of CSM is simple, but it cannot determine the fault category and is usually used to diagnose short circuit faults. CSM is suitable for fault diagnosis in small power plants, while the cost in large power plants is high.

5) Other non-electrical fault diagnosis methods, such as IIAM, are mainly used to diagnose HS and cracks. MMM is economical and applicable with a simple algorithm.

In conclusion, This paper provides a state-of-the-art guide for researchers and engineers in the field of PVS fault diagnosis. Through a detailed and comprehensive analysis of the various diagnostic methods, this paper offers insights and conclusions that can be employed in this field.

VI. Perspectives

The following six suggestions for future research can help overcome the limitations of existing diagnostic methods and provide more accurate and efficient fault diagnosis in PVS, especially in large PV power stations.

1) Improvement of the fault model for PVS. The existing diagnosis methods have their limitations in diagnosing faults in large PV power stations, which have numerous pieces of equipment and complex data to be detected. Therefore, the current PV fault model cannot accurately diagnose all faults, and the data analysis system cannot undertake such high work intensity. Work is needed to develop new failure models that can accurately diagnose complex and diverse faults in large PV power stations.

2) Addition of more measurement variables to improve diagnostic accuracy. Although most diagnosis methods are based on current and voltage waveform signals, temperature, and other measurement variables, they still have certain limitations and errors. Therefore, more measurement variables must be added to diagnose faults accurately.

3) Development of diagnostic methods that can diagnose more fault types. Current diagnostic procedures can only diagnose up to four to six faults, mostly related to aging, shielding, pollution, and delamination. However, the diagnosis methods for more serious flaws, such as LLF, GF, AF, and HSF, can only diagnose one. To address this issue, new diagnostic methods need to be developed to diagnose more fault types and reduce the need for multiple diagnosis systems.

4) Development of online fault diagnosis methods. Some diagnostic procedures can only be carried out when the PV power station is offline, which may affect some critical power supplies. Therefore, online diagnostic methods with an approximate range and real-time characteristics need to be developed.

5) Improvement of the original components of the PV system. Currently, measuring data for PV fault diagnosis generally requires specific equipment, which is expensive and requires regular maintenance. To reduce economic costs and make the planning of PV power stations more straightforward and more transparent, the original components need to be improved for data measurement.

6) Development of equipment for diagnosing PV faults. Currently, most PV components on the market are used to protect PVS from fault damage, such as series DC fault arc circuit breakers. However, it needs to be simplified and low cost for fault diagnosis. To solve this problem, new equipment specifically designed for diagnosing PV faults needs to be developed.

Acknowledgments

Not applicabie.

Authors' Contributions

Bo Yang: writing review and editing, writing original draft, and conceptualization. Ruyi Zheng: writing original draft and data curation. Yiming Han: writing review, editing and supervision. Jianxiang Huang: funding acquisition and formal analysis. Miwei Li: visualization and data curation. Shi Su: funding acquisition and formal analysis. Hongchun Shu: supervision and resources. Zhengxun Guo: visualization and data curation. All authors read and approved the final manuscript.

Funding

This work is supported by the National Natural Science Foundation of China (No. 61963020 and No. 62263014) and Yunnan Provincial Basic Research Project (No. 202401AT070344 and No. 202301AT070443).

Availability of Data and Materials

Please contact the corresponding author for data material request.

DECLARATIONS

Competing interests: The authors declare that they have no known competing financial interests or personal relationships that could have appeared to influence the work reported in this paper.

AUTHORS' INFORMATION

Bo Yang received the Ph.D. degree in University of Liverpool, UK. (Jointly sponsored by University of Liverpool and China Scholarship Council), in 2015. Dr. Yang is currently a professor with the School of Electrical Engineering, Kunming University of Science and Technology, Kunming, China. His research interests include intelligent optimization and control of renewable energy and energy storage system.

Ruyi Zheng received his B.Eng. degree in Kunming University of Science and Technology, Kunming, China, in 2023. She is currently pursuing a M.Sc degree in degree in Electronic Engineering from Kunming University of Science and Technology, Kunming, China. Her research interests include the prediction of photovoltaic cells.

Yiming Han received the B.Eng. degree in Kunming City College, Kunming, China, in 2015, and received the Ph.D. degree from Kunming University of Science and Technology, Kunming, China in 2021. His research interests include power system protection and fault location, micro-grid automation, and renewable energy.

Jianxiang Huan received her B.Eng. degree in Central South University, Changsha, China. She is currently working in the Kunming Bureau of CSG EHV Transmission Company, Kunming, China. Her research interests include renewable energy optimization and control.

Miwei Li received his B.Eng. degree in Shaanxi University of Technology, Hanzhong, China, in 2023. She is currently pursuing a M.Sc degree in electronic engineering from Kunming University of Science and Technology, Kunming, China. Her research interests include the optimization of wave energy system array.

Hongchun Shu received the Ph.D. degree from Harbin Institute of Technology, Harbin, China, in 1997. Dr. Shu is currently a professor with the School of Electrical Engineering, Kunming University of Science and Technology, Kunming, China. His research interests include power line traveling wave fault ranging and lightning strike station end detection and analysis technology.

Shi Su received his B.Eng. degree in Central South University, Changsha, China. He is currently working in the Power Science Research Institute of Yunnan Power Grid Co., Ltd, Kunming, China. His research interests include renewable energy optimization and control.

Zhengxun Guo received his M.Sc degree in Kunming University of Science and Technology, Kunming, China, in 2023. He is currently pursuing the doctoral degree in Electrical Engineering from Northeastern University, Shenyang, China. His research interests include renewable energy optimization and control.

REFERENCES

[1] B. Yang, Y. Li, and J. Li *et al*., "Comprehensive summary of solid oxide fuel cell control: a state-of-the-art review," *Protection and Control of Modern Power Systems*, vol. 7, no. 3, pp. 1-31, Jul. 2022.

[2] B. Yang, B. Liu, and H. Zhou *et al*., "A critical survey of technologies of large offshore wind farm integration: summary, advances, and perspectives," *Protection and Control of Modern Power Systems*, vol. 7, no. 2, pp. 1-3, Apr. 2022.

[3] Y. Chen, B. Yang, and Z. Guo *et al*., "Dynamic reconfiguration for TEG systems under heterogeneous temperature distribution via adaptive coordinated seeker," *Protection and Control of Modern Power Systems*, vol. 7, no. 3, pp. 1-18, Jul. 2022.

[4] Y. Wang and B. Yang, "Optimal PV array reconfiguration under partial shading condition through dynamic leader based collective intelligence," *Protection and Control of Modern Power Systems*, vol. 8, no. 3, pp. 1-16, Jul. 2023.

[5] P. K. Guchhait and A. Banerjee, "Stability enhancement of wind energy integrated hybrid system with the help of static synchronous compensator and symbiosis organisms search algorithm," *Protection and Control of Modern Power Systems*, vol. 5, no. 2, pp. 1-13, Apr. 2020.

[6] B. Yang, T. Yu, and X. Zhang *et al*., "Dynamic leader based collective intelligence for maximum power point tracking of PV systems affected by partial shading condition," *Energy Conversion and Management*, vol. 179, pp. 286-303, Jan. 2019.

[7] H. Ming, B. Xia, and K. Y. Lee *et al*., "Prediction and assessment of demand response potential with coupon incentives in highly renewable power systems," *Protection and Control of Modern Power Systems*, vol. 5, no. 2, pp. 1-14, Apr. 2020.

[8] X. He, L. Chu, and R. C. Qiu *et al*., "Invisible units detection and estimation based on random matrix theory," *IEEE Transaction on Power Systems*, vol. 35, no. 3, pp. 1846-1855, May 2020.

[9] B. Wang, Y. Wu, and P. Liu *et al*., "Regional heterogeneity governing renewable energy development-from the perspective of industrial chain of production, transportation and consumption," *Journal of Beijing Institute of Technology (Social Sciences Edition)*, vol. 24, no. 1, pp. 39-50, Oct. 2020. (in Chinese)

[10] J. Li, K. Jiang, and X. Dong *et al*., "Active power control strategy for a photovoltaic DC grid-connected system based on power self feedback iteration in an AC fault," *Power System Protection and Control*, vol. 51, no. 23, pp. 37-44, Dec. 2022. (in Chinese)

[11] M. K. Alam, F. Khan, and J. Johnson *et al*., "A comprehensive review of catastrophic faults in PV arrays: Types, detection, and mitigation techniques," *IEEE Journal of Photovoltaics*, vol. 5, no. 3, pp. 982-997, May 2015.

[12] A. Y. Appiah, X. H. Zhang, and B. B. K. Ayawli *et al*., "Review and performance evaluation of photovoltaic array fault detection and diagnosis techniques," *International Journal of Photoenergy*, vol. 2019, pp. 1-19, Jan. 2019.

[13] M. V. Daria, W. Jan, and U. Dan *et al*., "Fire hazard associated with different types of photovoltaic power plants: effect of vegetation management," *Renewable and Sustainable Energy Reviews*, vol. 162, May 2022.

[14] X. Wang, S. Hao, and Z. Zhang *et al*., "Research and application of fire pre-alarm system of precision photovoltaic power station based on end-edge-cloud architecture," *Power System Engineering*, vol. 37, no. 6, pp. 72-74, 78, Oct. 2021. (in Chinese)

[15] H. Al-Sheikh and N. Moubayed, "Fault detection and diagnosis of renewable energy systems: an overview," in *2012 International Conference on Renewable Energies for Developing Countries (REDEC)*, Beirut, Lebanon, Nov. 2012, pp. 1-7.

[16] S. Li, Y. Yan, and F. Xiang *et al*., "A comprehensive review on detection method for DC fault arc in photovoltaic system," *Journal of Electrical Engineering*, vol. 61, no. 2, pp. 10-16, Feb. 2023. (in Chinese)

[17] X. Zhang and Z. Li, "A survey on photovoltaic array fault diagnosis algorithms," *Electrical Measurement and Instrumentation*, vol. 12, no. 2, pp. 143-147, Feb. 2022. (in Chinese)

[18] A. Mellit, G. M. Tina, and S. A. Kalogirou, "Fault detection and diagnosis methods for photovoltaic systems: a review," *Renewable and Sustainable Energy Reviews*, vol. 91, pp. 1-17, Aug. 2018.

[19] J. Tang, L. Peng, and Z. Zhang *et al*., "Discoloration analysis on photovoltaic EVA," *Synthetic Materials Aging and Application*, vol. 40, no. 6, pp. 30-38, Dec. 2011. (in Chinese)

[20] F. J. Pern, "Ethylene-vinyl acetate (EVA) encapsulants for photovoltaic modules: degradation and discoloration mechanisms and formulation modifications for improved photostability," *Angewandte Makromolekulare Chemie*, vol. 252, pp. 195-216, Jun. 1997.

[21] P. Cornelia, P. Lea, and W. Karl-Ander *et al*., "Towards the origin of photochemical EVA discoloration," in *2013 IEEE 39th Photovoltaic Specialists Conference (PVSC)*, Tampa, USA, Jun. 2013, pp. 1579-1584.

[22] X. Jiang, W. He, and J. Yang *et al*., "Study on UV induced EVA discoloration for crystalline silicon solar modules," in *2018 IEEE 7th World Conference on Photovoltaic Energy Conversion (WCPEC)*, Waikoloa, USA, Jun. 2018, pp. 1282-1285.

[23] A. Sinha and R Gupta, "Effects of different excitation waveforms on detection and characterisation of delamination in PV modules by active infrared thermography," *Nondestructive Testing and Evaluation*, vol. 32, no. 4, pp. 418-434, Oct. 2017.

[24] A. Sinha, O.S. Sastry, and R. Gupta, "Detection and characterisation of delamination in PV modules by active infrared thermography," *Nondestructive Testing and Evaluation*, vol. 31, no. 1, pp. 1-16, Jan. 2016.

[25] M. R. Maghami, H. Hizam, and C. Gomes *et al*., "Power loss due to soiling on solar panel: a review," *Renewable and Sustainable Energy Reviews*, vol. 59, pp. 1307-1316, Jun. 2016.

[26] M. Simon and E. L. Meyer, "Detection and analysis of hot-spot formation in solar cells," *Solar Energy Materials and Solar Cells*, vol. 94, no. 2, pp. 106-113, Jun. 2019.

[27] K. A. Kim and P. T. Krein, "Reexamination of photovoltaic hot spotting to show inadequacy of the bypass diode," *IEEE Journal of Photovoltaics*, vol. 5, no. 5, pp. 1435-1441, Jan. 2015.

[28] K. A. Kim, G. S Seo, and B. H. Cho *et al*., "Photovoltaic hot-spot detection for solar panel substrings using AC parameter characterization," *IEEE Transactions on Power Electronics*, vol. 31, no. 2, pp. 1121-1130, Feb. 2016.

[29] R. Moret, E. Lorenzo, and L. Narvarte, "Experimental observations on hot-spots and derived acceptance/rejection criteria," *Solar Energy*, vol. 118, pp. 28-40, Aug. 2015.

[30] W. Luo, Y. S. Khoo, and P. Hacke *et al*., "Potential-induced degradation in photovoltaic modules: a critical review," *Energy and Environmental Science*, vol. 10, no.1, pp. 43-68, Jan. 2017.

[31] D.R. Gong, Y.N. Chen, and G. Sun *et al*., "Research on potential induced degradation (PID) of PV modules in different typical climate regions," in *International Conference on Recent Advances in Materials, Mechanical and Civil Engineering (ICRAMMCE)*, Hyderabad, India, Jun. 2017, pp. 1-5.

[32] Y. Du, "Influence of photovoltaic module PID problem on photovoltaic power generating capacity," *Energy and Energy Conservation*, no. 10, pp. 34-36, Oct. 2021. (in Chinese)

[33] Z. Shen, X. Zhang, and X. Jiang *et al*., "Research on potential induced degradation of PV modules," *Chinese Journal of Power Sources*, vol. 40, no. 6, pp. 1327-1329, Jun. 2016. (in Chinese)

[34] A. Triki-Lahiani, A. B. Abdelghani, and I. Slama-Belkhodja, "Fault detection and monitoring systems for photovoltaic installations: a review," *Renewable and Sustainable Energy Reviews*, vol. 82, pp. 2680-2692, Feb. 2018.

[35] J. Lindroos and H. Savin, "Review of light-induced degradation in crystalline silicon solar cells," *Solar Energy Materials and Solar Cells*, vol. 147, pp. 115-126, Apr. 2016.

[36] T. Gunda, S. Hackett, and L. Kraus *et al*., "A machine learning evaluation of maintenance records for common failure modes in PV inverters," *IEEE Access*, vol. 8, pp. 211610-211620, Dec. 2020.

[37] M. J. Sathik, J. D. Navamani, and A. Lavanya *et al*., "Reliability analysis of power components in restructured DC/DC converters," *IEEE Transactions on device*

and materials reliability, vol. 21, no. 4, pp. 544-555, Dec. 2021.

[38] S. Yang, D. Xiang, and A. Bryant *et al*., "Condition monitoring for device reliability in power electronic converters: a review," *IEEE Transactions on Power Electronics*, vol. 25, no.11, pp. 2734-2752, Nov. 2010.

[39] G. Wang, J. Bai, and S. Liu *et al*., "Development of anti-shadow occlusion intelligent control junction box," *Acta Energiae Solaris Sinica*, vol. 42, no. 2, pp. 425-430, Feb. 2021. (in Chinese)

[40] N.G. Dhere, N. Shiradkar, and E. Schneller *et al*., "The reliability of bypass diodes in PV modules," in *Conference on Reliability of Photovoltaic Cells, Modules, Components, and Systems VI*, San Diego, USA, Aug. 2013, pp. 1-8.

[41] N.S. Shiradkar, E. Schnellerl, and N.G. Dherel *et al*., "Predicting thermal runaway in bypass diodes in photovoltaic modules," in *2014 IEEE 40th Photovoltaic Specialist Conference (PVSC)*, Denver, USA, Jun. 2014, pp. 3585-3588.

[42] K. A. Saleh, A. Hooshyar, and E. E. El-Saadany *et al*., "Voltage-based protection scheme for faults within utility-scale photovoltaic arrays," *IEEE Transactions on Smart Grid*, vol. 9, no. 5, pp. 4367-4382, Sept. 2018.

[43] M. K. Alam and F. Khan, "PV ground-fault detection using spread spectrum time domain reflectometry (SSTDR)," in *2013 IEEE Energy Conversion Congress and Exposition (ECCE)*, Denver, UAS, Sept. 2013, pp. 1015-1020.

[44] Y. Zhao, J. F. D. Palma, and J. Mosesian *et al*., "Line-line fault analysis and protection challenges in solar photovoltaic arrays," *IEEE Transactions on Industrial Electronics*, vol. 60, no. 9, pp. 3784-3795, Jan. 2013.

[45] A. Eskandari, J. Milimonfared, and M Aghaei, "Line-line fault detection and classification for photovoltaic systems using ensemble learning model based on I-V characteristics," *Solar Energy*, vol. 211, pp. 354-365, Nov. 2020.

[46] W. Miao, K. H. Lam, and P. W. T. Pong, "A string-current behavior and current sensing-based technique for line-line fault detection in photovoltaic systems," *IEEE Transactions on Magnetics*, vol. 57, no. 2, pp. 1-6, Feb. 2021.

[47] D. S. Pillai and R. Natarajan, "A compatibility analysis on NEC, IEC, and UL standards for protection against line-line and line-ground faults in PV arrays," *IEEE Journal of Photovoltaics*, vol. 9, no. 3, pp. 864-871, May 2019.

[48] S. Lu, B. T. Phung, and D. M. Zhang, "A comprehensive review on DC arc faults and their diagnosis methods in photovoltaic systems," *Renewable and Sustainable Energy Reviews*, vol. 89, pp. 88-98, Jun. 2018.

[49] X. Yao, L. Herrera, and L. Yue *et al*., "Experimental study of series DC arc in distribution systems," in *2018 IEEE Energy Conversion Congress and Exposition (ECCE)*, Portland, USA, Sept. 2018, pp. 3713-3718.

[50] R. Li, Q. Xiong, and C. Zhang *et al*., "Arc fault detection in photovoltaic systems based on pseudo Wigner-Ville distributed algorithm," in *3rd International Conference on Smart Power and Internet Energy Systems (SPIES)-Towards A Sustainable and Affordable Energy Transition*, Shanghai, China, Sept. 2021, pp. 118-122.

[51] I. C. Kim, B. Lehman, and R. Ball, "A series DC arc fault detection algorithm based on PV operating characteristics and detailed extraction of pink noise behavior," in *2021 Thirty-Sixth Annual IEEE Applied Power Electronics Conference and Exposition (APEC)*, Phoenix, AZ, Jun. 2021, pp. 989-994.

[52] T. Takashima, J. Yamaguchi, and K. Otani *et al*., "Experimental studies of fault location in PV module strings," *Solar Energy Materials and Solar Cells*, vol. 93, no. 6-7, pp. 1079-1082, Dec. 2007.

[53] Z. Yan, "Research on SSTDR-based cable fault detection and location system," M.S. thesis, Electronic and Communications Engineering, Xi'an University of Technology, Shanxi, China, 2022. (in Chinese)

[54] L. Schirone, F. Califano, and U. Moschella *et al*., "Fault finding in a 1 MW photovoltaic plant by reflectometry," in *Proceedings of the 24th IEEE Photovoltaic Specialist on Energy Conversion*, Waikoloa, HI, Dec. 1994, pp. 846-849.

[55] M. K. Alam, F. Khan, and J. Johnson *et al*., "PV arc-fault detection using spread spectrum time domain reflectometry (SSTDR)," in *2014 IEEE Energy Conversion Congress and Exposition (ECCE)*, Pittsburgh, USA, Sept. 2014, pp. 3294-3300.

[56] Q. Li and F. H. Khan, "Identifying natural degradation/aging in power MOSFETs in a live grid-tied PV inverter using spread spectrum time domain reflectometry," in *International Power Electronics Conference (IPEC-ECCE-ASIA)*, Hiroshima, Japan, May 2014, pp. 2161-2166.

[57] N. K. T. Jayakumar, M. U. Saleh, and E. Benoit, "Fault detection in PV strings using SSTDR," in *2018 USNC-URSI Radio Science Meeting (Joint With AP-S Symposium)*, Boston, USA, Jul. 2018, pp: 9-10.

[58] A. S. Edun, S. Kingston, and C. LaFlamme *et al*., "Detection and localization of disconnections in a large-scale string of photovoltaics using SSTDR," *IEEE Journal of Photovoltaics*, vol. 11, no. 4, pp. 1097-1104, Jul. 2021.

[59] M. U. Saleh, C. Deline, and E. J. Benoit *et al*., "Detection and localization of damaged photovoltaic cells and modules using spread spectrum time domain reflectometry," *IEEE Journal of Photovoltaics*, vol. 11, no. 1, pp. 195-201, Jan. 2021.

[60] L. C, LaFlamme, E. Benoit, and A. Edun *et al*., "Quantifying the environmental sensitivity of SSTDR signals for monitoring PV strings," *IEEE Journal of Photovoltaics*, vol. 12, no.1, pp. 381-387, Jan. 2022.

[61] Y. Erkaya, I. Flory, and S. X. Marsillac, "Development of a string level I-V curve tracer," in *2014 IEEE 40th Photovoltaic Specialist Conference (PVSC)*, Denver, USA, Jun. 2014, pp. 3104-3107.

[62] H. Kaeamura, K. Naka, and N. Yonekura *et al*., "Simulation of I-V characteristics of a PV module with shaded PV cells," *Fuel and Energy Abstracts*, vol. 44, no. 4, pp. 613-621, Feb. 2003.

[63] A. Al-Subhi, I. El-Amin, and M. I. Mosaad, "Efficient predictive models for characterization of photovoltaic module performance," S*ustainable Energy Technologies and Assessments*, vol. 38, no. C, Apr. 2020.

[64] N. D. Tuyen, L. V. Thinh, and V. X. S. Huu *et al*., "Forecasting I-V characteristic of PV modules considering real operating conditions using numerical method and deep learning," in *2020 International Conference on Smart Grids and Energy Systems (SGES)*, Electrical Network, Nov. 2020, pp. 544-549.

[65] M. Ma, Z. Zhang, and Z. Xie *et al*., "Fault diagnosis of cracks in crystalline silicon photovoltaic modules through I-V curve," *Microelectronics Reliability*, vol. 114, Nov. 2020.

[66] M. Ma, H. Liu, and Z. Zhang *et al*., "Rapid diagnosis of hot spot failure of crystalline silicon PV module based on I-V curve," in *30th European Symposium on Reliability of Electron Devices, Failure Physics and Analysis (ESREF)*, Toulouse, France, Sept. 2019.

[67] Z. Zhang, M. Ma, and W. Ma *et al*., "A data-driven photovoltaic string current mismatch fault diagnosis method based on I-V curve," *Microelectronics Reliability*, vol. 138, Nov. 2022.

[68] M. Ma, H. Wang, and N. Xiang *et al*., "Fault diagnosis of PID in crystalline silicon photovoltaic modules through I-V curve," *Microelectronics Reliability*, vol. 126, pp. 114236, Nov. 2021.

[69] M. Ming, Z. Zhang, and H. Liu *et al*., "Fault diagnosis of crystalline silicon photovoltaic module based on I-V characteristic analysis," *Acta Energiae Solaris Sinica*, vol. 42, no. 6, pp. 130-137, Sept. 2021. (in Chinese)

[70] B. P. Kumar, R. Nitheesh, and M. Cjakkarapani, "Estimation of PV module degradation through extraction of I-V curve at inverter pre-startup condition," *IET Renewable Power Generation*, vol. 14, no. 17, pp. 3479-3486, Dec. 2020.

[71] T. Mishina, H. Kawamura, and S. Yamanaka *et al*., "A study of the automatic analysis for the I-V curves of a photovoltaic subarray," in *29th IEEE Photovoltaic Specialists Conference*, New Orleans, USA, May 2022, pp. 1630-1633.

[72] J. Huang, R. Wai, and G. Yang, "Design of hybrid artificial bee colony algorithm and semi-supervised extreme learning machine for PV fault diagnoses by considering dust impact," *IEEE Transactions on Power Electronics*, vol. 35, no. 7, pp. 7086-7099, Jul. 2020.

[73] L. Cao, W. Song, and R. Han, "Fault diagnosis in solar photovoltaic grid-connected power system based on fault tree," *Electrical Engineering*, no. 4, pp. 36-37, 64, Apr. 2012. (in Chinese)

[74] Z. Li, Z. Ye, and B. Wang, "Sensor fault diagnosis based on wavelet analysis and neura network," *Machine Building & Automation*, vol. 52, no. 4, pp. 196-201, Aug. 2023. (in Chinese)

[75] Y. Liu, Y. Zhao, and L. Zhang *et al*., "Photovoltaic power forecasting based on wavelet packet decomposition of long short-term memory network," *Computer & Digital Engineering*, vol. 50, no. 9, pp. 2114-2118, Feb. 2022. (in Chinese)

[76] Y. Wang, C. Wu, and D. Zhou *et al*., "A survey of fault diagnosis for PV array based on BP neural network," *Power System Protection and Control*, vol. 41, no. 16, pp. 108-114, Aug. 2013. (in Chinese)

[77] B. Yang, J. Wang, and L. Yu *et al*., "A critical survey on proton exchange membrane fuel cell parameter estimation using meta-heuristic algorithms," *Journal of Cleaner Production*, vol. 265, Aug. 2020.

[78] H. Shen, Z. Wang, and C. Gao *et al*., "Determining the number of BP neural network hidden layer units," *Journal of Tianjin University of Technology*, vol. 24, no. 5, pp. 13-15, Oct. 2008. (in Chinese)

[79] D. Li, L. Xu, and D. Long *et al*., "Photovoltaic array fault diagnosis with genetic algorithm optimized BP neural network," *Microprocessors*, vol. 42, no. 6, pp. 23-26, Dec. 2021. (in Chinese)

[80] G. He, J. Zhou, and J. Zhou *et al*., "Research on fault diagnosis method of photovoltaic array based on BP neural network with adaptive weight particle swarm optimization," *Electronic Design Engineering*, vol. 29, no. 9, pp. 75-79, May 2021. (in Chinese)

[81] J. Ma, Z. Zhao, and Q. Zhang, "Fault diagnosis of photovoltaic modules based on improved RBF neural network," *Electrical Measurement and Instrumentation*, vol. 58, no. 2, pp. 118-124, Jul. 2021. (in Chinese)

[82] J. Liu and S. Wang, "Research on fault diagnosis of PV array based on PNN," *Journal of Heilongjiang University of Technology*, vol. 21, no. 10, pp. 76-82, Oct. 2021. (in Chinese)

[83] W. Zhang, Y. Lin, and J. Li *et al*., "Fault identification for photovoltaic power generation system based on long short-term memory," *Thermal Power Generation*, vol. 50, no. 6, pp. 60-68, Feb. 2021. (in Chinese)

[84] T. Chen, R. Wang, and X. Fan *et al*., "Photovoltaic fault diagnosis using art neural network based on wavelet feature," *Power Electronics*, vol. 56, no, 8, pp. 81-84, 118, Aug. 2022. (in Chinese)

[85] L. Li, X. Zhang, and Z. Wang, "Fault diagnosis in solar photovoltaic grid-connected power system based on fault tree and BAM neural network," *Transactions of China Electrotechnical Society*, vol. 30, no. 2, pp. 248-254, Jan. 2015. (in Chinese)

[86] Z. Wang and R. S. Balog, "Arc fault and flash detection in photovoltaic systems using wavelet transform and support vector machines," in *43rd IEEE Photovoltaic Specialists Conference (PVSC)*, Portland, USA, Jun. 2016, pp. 3275-3280.

[87] W. Rezgui, L. H. Mouss, and N. K. Mouss *et al*., "A smart algorithm for the diagnosis of short-circuit faults in a photovoltaic generator," in *1st International Conference on Green Energy (ICGE)*, Sfax, Tunisia, Mar. 2014, pp. 139-143.

[88] P. Chu, Z. He, and K. Zhang *et al*., "Series DC arc fault detection in photovoltaic system based on multi-feature fusion and SVM," in *11th International Conference on Power and Energy Systems (ICPES)*, Shanghai, China, Dec. 2021, pp. 436-441.

[89] M. M. Badr, M. S. Hamad, and A. S. Abdel *et al*., "Fault detection and diagnosis for photovoltaic array under grid connected using support vector machine," in *IEEE Conference on Power Electronics and Renewable Energy (IEEE CPERE)*, Aswan, Egypt, Oct. 2019, pp. 546-553.

[90] H. Guo and Z. Li, "Research on fault diagnosis of photovoltaic array based on support vector machine optimized by genetic algorithm," *Intelligent Computer and Applications*, vol. 9, no. 5, pp. 58-62, Oct. 2019. (in Chinese)

[91] P. Lin, Z. Chen, and L. Wu *et al*., "Fault detection and classification for photovoltaic arrays based on PSO-SVM," *Journal of Fuzhou University (Natural Science Edition)*, vol. 45, no. 5, pp. 652-658, Oct. 2017. (in Chinese)

[92] K. Liu, T. Li, and D. Liu *et al*., "Fault diagnosis of PV array based on ABC-SVM algorithm," *Chinese Journal of Power Sources*, vol. 45, no. 9, pp. 1171-1174, Sept. 2021. (in Chinese)

[93] P. Sun, T. Chen, and C. Cheng *et al*., "Research on fault diagnosis of photovoltaic array based on SOA-SVM model," *Journal of Power Supply*, pp. 1-13, Aug. 2022. (in Chinese)

[94] C. Wu, D. Zhou, and Z. Li *et al*., "Hot spot detection and fuzzy optimization control method of PV module," *Proceedings of the CSEE*, vol. 33, no. 36, pp. 20-61, Dec. 2013. (in Chinese)

[95] R. Bi, M. Ding, and Z. Xu *et al*., "PV array fault diagnosis based on FCM," *Acta Energiae Solaris Sinica*, vol. 37, no. 3, pp. 730-736, Mar. 2016. (in Chinese)

[96] Z. Wei, A. Li, and S. Shao *et al*., "Fault diagnosis of PV array based on FCM-FM algorithm," *Advances in New and Renewable Energy*, vol. 6, no. 4, pp. 297-303, Aug. 2018. (in Chinese)

[97] Y. Wang, T. Yan, and F. Chen *et al*., "Fault diagnosis of photovoltaic modules based on combination of FCM and SRF," *Chinese Journal of Power Sources*, vol. 43, no. 12, pp. 2009-2013，2057, Dec. 2019. (in Chinese)

[98] H. Yu, Y. Liu, and H. Wang *et al*., "A DC side fault location method for PV power station based on 3σ criterion and FCM algorithm," *Solar Energy*, vol. 298, no. 2, pp. 50-55, Feb. 2019. (in Chinese)

[99] G. Zhang, R. Zhao, and Y. Wang, "Study on arc fault detection method of photovoltaic system based on FCM," *High Voltage Apparatus*, vol. 58, no. 5, pp. 15-22, May 2022. (in Chinese)

[100] S. Liu, L. Dong, and X. Wang *et al*., "Photovoltaic array fault diagnosis based on GKFCM," Acta Energiae Solaris Sinica, vol. 42, no. 5, pp. 286-294, May 2021. (in Chinese)

[101] J. Sun, L. Li, and G. Li *et al*., "Overview of PV modules, fault diagnosis, technology," *Solar Energy*, vol. 24, no. 2, pp. 131-136, Feb. 2010. (in Chinese)

[102] Y. Wu, T. Li, and J. Qiao *et al*., "Analysis of sensor placement in photovoltaic array fault location," *Telecom Power Technology*, vol. 34, no. 5, pp. 50-51, Sept. 2017. (in Chinese)

[103] W. Song, T. Li, and J. Qiao *et al*., "Research on fault detection method of TCT structured photovoltaic array," *Chinese Journal of Power Sources*, vol. 43, no. 7, pp. 1164-1167, Jul. 2019. (in Chinese)

[104] Z. Cheng, B. Li, and L. Li *et al*., "A fault detection method for new PV module strufure," *Journal of Electronic Measurement and Instrumentation*, vol. 24, no. 2, pp. 131-136, Feb. 2010. (in Chinese)

[105] M. Alajmi, K. Awedat, and M. S. Aldeen *et al*., "IR thermal image analysis: An efficient algorithm for accurate hot-spot fault detection and localization in solar photovoltaic systems," in *IEEE International Conference on Electro Information Technology (EIT)*, Brookings, USA, May 2019, pp. 162-168.

[106] Y. He, B. Du, and S. Huang, "Noncontact electromagnetic induction excited infrared thermography for photovoltaic cells and modules inspection," *IEEE Transactions on Industrial Informatics*, vol. 14, no. 12, pp. 5585-5593, Dec. 2018.

[107] W. Fu, L. Zhou, and K. Guo *et al*., "Research on engineering analytical model of solar cells," *Transactions of China Electrotechnical Society*, vol. 26, no. 10, pp. 211-216, Jan. 2011. (in Chinese)

[108] A. C. M. Soares and E. Vieira, M. M. Casaro, "Simulation of a photovoltaic model using bisection method," in *11th Brazilian Power Electronics Conference (COBEP)*, Natal, Brazil, Sept. 2011, pp. 807-811.

[109] S. A. Mahmoud and H. N. Mahmoud, "Novel modeling approach for photovoltaic arrays," in *55th IEEE International Midwest Symposium on Circuits and Systems (MWSCAS)*, Boise, USA, Aug. 2012, pp. 790-793.

[110] S. Madi and A. Kheldoun, "Bond graph based modeling for parameter identification of photovoltaic module," *Energy*, vol. 141, pp. 1456-1465, Dec. 2017.

[111] M. Dyvak, K. Gorecki, and J. Zarebski *et al*., "Mathematical model of weather conditions influence on properties of photovoltaic installation and method of its identification," in *9th International Conference on Advanced Computer Information Technologies (ACIT)*, Ceske Budejovice, Czech Republic, Jun. 2019, pp. 35-39.